Benha University

Faculty of Engineering

Improving Digital Signaling on Time Varying Channels using RAKE Receiver

by

Eng. Amal Sabry Faragalla

A thesis submitted
in partial fulfillment of the requirements for the degree of
Master of Science in
Electrical Engineering Technology

Supervised by

Prof. Dr. Abdel Halim Zekry
Electronics and Communications Engineering Department
Faculty of Engineering
Ain Shams University

Dr. Ayman Mustafa Hassan
Electrical Engineering Department
Faculty of Engineering
Benha University

Dr. Hossam El-Din El Sayed
Electrical Engineering Department
Faculty of Engineering
Benha University

September 2013

The undersigned have examined the thesis entitled '**Improving Digital Signaling on Time Varying Channels using RAKE Receiver**' presented by **Amal Sabry Faragalla**, a candidate for the degree of **Master of Science in Electrical Engineering technology** and hereby certify that it is worthy of acceptance.

Approved by the Examining Committee:

Prof. Abdulhalim Abdulnaby Zekry, Ain Shams University

Thesis Advisor and Committee Chairperson

Prof. Talaat Abdullatif Elgarf, Higher Technological Institute

Examiner

Prof. Salah Ghazy Ramadan, Benha University

Examiner

Accepted for Electrical Engineering Department:

Prof. Mahmoud Elbahy

Department Chairman

Accepted for the Post Graduate Affairs:

Prof. Hesham Elbatsh

Vice Dean for post graduate studies

Accepted for the Faculty:

Prof. Mohammed Basiouny

Dean of the Faculty of Engineering

Abstract

In the radio environment, transmitted signals arrive at the receiver via a direct, unobstructed path or via multiple paths from the reflection, diffraction and scattering of surrounding objects such as buildings and trees. This multipath propagation causes the signal at the receiver to distort and fade significantly, leading to inter-symbol interference (ISI). Spread spectrum mobile communication systems use RAKE receivers to minimize these communication errors resulting from multipath effects.

The aim of this thesis is to develop a MATLAB model of a spread spectrum system using RAKE receiver and evaluating its performance in a time varying channel. A DS-SS system with a BPSK modulation is first introduced and evaluated in AWGN and multipath fading channels with and without Rake receiver. This was performed under different conditions like using different spreading codes and using different number of rake fingers. Ideally, the number of correlators in the RAKE receiver should match the number of multipath signals. The effect of multipath delay spread is then investigated by using different combinations of predefined delays for the multipath channel. The next step was to provide channel estimation using LMS filter for a stationary channel and testing different pilot signals with different lengths. Finally, a complete system was introduced with a time varying channel and tested at different rates of change. The performance of the simulated system is evaluated through the BER calculation by Monte Carlo analysis and theoretical analysis supported by MATLAB (v.7.8).

Acknowledgements

A long way has passed until this moment; a way that was full of many ups and downs. And finally, it is the time to thank all those who have contributed to this final outcome.

First of all, I would like to thank **GOD** for giving me the capability to learn all what I have learned in my life and to give me the ability to write this thesis.

After GOD, I grant all the success realized in my life to **my parents** to whom I owe all good things I learned and will learn till I die.

Also I would like to dedicate this acknowledgement to all the people who helped me making it happen especially for **my husband** for his continuous support and understanding without which I have probably quitted a long time ago, **my 2 daughters** who sacrificed many happy moments I had to be busy away from them. I'm also grateful to all **my family** and **my dear friends** for their support and continuous help all the way long.

I also want to express my gratitude to **Prof. Dr. Abdel Halim Zekry** who's not only served as my supervisor but also encouraged me and provided me with valuable guidance and indispensable help. His words of advice, his trust, and his patience and understanding helped me to finish this work. He has been a role model to me.

And finally, special thanks to my supervisors **Dr. Ayman Mustafa Hassan** and **Dr. Hossam Eldin Elsayed** for their support till finalizing this research.

It is always impossible to personally thank everyone who has facilitated successful completion of this thesis. To those of you who I didn't specifically name, I also give my thanks for moving me towards my goal.

Contents

List of Figures

List of Tables

List of Symbols

τ	Time delay
α	Amplitude level
$\acute{O}$	Phase shift
C	Capacity of a communication channel
B	Channel bandwidth
Bs	Information bandwidth
P_G	Processing gain
S	Signal power
N	Noise power
M	Number of flip flops
$R_a\,(\tau)$	Auto-correlation function
$R_c\,(\tau)$	Cross-correlation function
T_b	Symbol period
T_c	Chip period
N	Sequence length
c_i	Feedback connection coefficient
L	Simple shift register length
E_b	Energy of a bit
N_o	Spectral energy of noise
θ_i	The phase of the ith branch of a linear combiner
α_i	Co-phasing factor

γ_0	The minimum SNR required for acceptable performance
$\overline{P_s}$	The average error probability
P_{out}	The outage probability
$P_s(\gamma_\Sigma)$	The probability of symbol error for demodulation of $s(t)$ in AWGN with SNR γ_Σ
$p_{\gamma_\Sigma}(\gamma)$	Probability distribution of random variable γ_Σ
μ	The step size factor

List of Acronyms

LOS	Line-of-Sight
ISI	Inter-Symbol Interference
AWGN	Additive White Gaussian Noise
WCDMA	Wideband Code Division Multiple Access
ASIC	Application-Specific Integrated Circuit
VHDL	VHSIC Hardware Description Language
CMOS	Complementary Metal–Oxide–Semiconductor
FPGA	Field-Programmable Gate Aarray
HDL	Hardware Description Language
MIMO	Multiple-Input/Multiple-Output
DSSS	Direct Sequence Spread Spectrum
BER	Bit Error Rate
RLS	Recursive Least Squares
UWB	Ultra Wide Band
DFE	Decision-Feedback Equalizer
MRC	Maximum Ratio Combiner
LMS	Least Mean Square
SNR	Signal-to-Noise Ratio
WSSUS	Wide-Sense Stationary Uncorrelated Scattering
PDPs	Power Delay Profiles
MPMC	Maximum Power Minimum Correlation
DSCDMA	Direct Sequence Code Division Multiple Access System
MAI	Multiple Access Interference
SI	Signature-Interleaved

P-Rake	Partial Rake
S-Rake	Selective Rake
A-rake	All Rake
SIC	Successive Interference Cancellation
LPI	Low Probability of Intercept
MMSE	Minimum Mean Square Error
G-RAKE	Generalized RAKE
LMMSE	Linear Minimum Mean Square Error
HSDPA	High-speed downlink packet access
SINR	Signal to Interference and Noise Ratio
MWP	Maximum Weight Placement
SoC	System-on-Chip
CORDIC	Coordinate Rotation Digital Computer
DS-UWB	Direct Sequence Ultra-Wideband
CE	Channel Estimator
HPS	Hybrid Partial/Selective
CSI	Channel State Information
MC-CDMA	Multi-Carrier Code Division Multiple Access
ISM	Industrial, Scientific and Medical
FH-SS	Frequency-Hopping Spread Spectrum
TH-SS	Time-Hopping Spread Spectrum
PN	Pseudo-Noise

SSRG	Simple Shift Register Generator
M-sequence	Maximum-Length Sequence
IS-95	Interim Standard 95
PSK	Binary Phase Shift Keying
NRZ	Non Return to Zero
DS/BPSK	Direct-Sequence Binary Phase Shift Keyed
SC	Selection Combining
I.I.D	Independent and Identically Distributed
SSC	Switch and Stay Combining
EGC	Equal Gain Combining
LAN	Local Area Network
SF	Spreading Factor

Chapter 1: Introduction

(1-1) Overview

Wireless communication has proved to be vital in our daily lives. However, the performance of the wireless communication systems is often limited or corrupted due to the nature of the mobile radio channel. In an urban environment, the transmission path between the transmitter and the receiver is severely obstructed by buildings and trees. Hence, a transmitted signal may travel through a direct line-of-sight (LOS) path and many multiple paths depending on the characteristics of the radio channel. Unlike wired channels that are stationary and predictable, radio channels are extremely random and difficult to model.

In general, a signal transmitting in a channel experiences two types of fading:

(1) Large-scale fading.
(2) Small-scale fading.

The mechanisms behind these two fading types are diverse, but can generally be attributed to reflection, diffraction and scattering [1]. These three propagation mechanisms are illustrated in fig. (1-1). Other transmission impairments in the wireless channel include free space loss, thermal noise and atmospheric absorption [2].

We will focus mainly on the three propagation mechanisms that cause the occurrence of small-scale multipath fading. The concept of how a RAKE receiver can be implemented to recover the time-dispersed signals in a multipath channel is explained later in chapter 3.

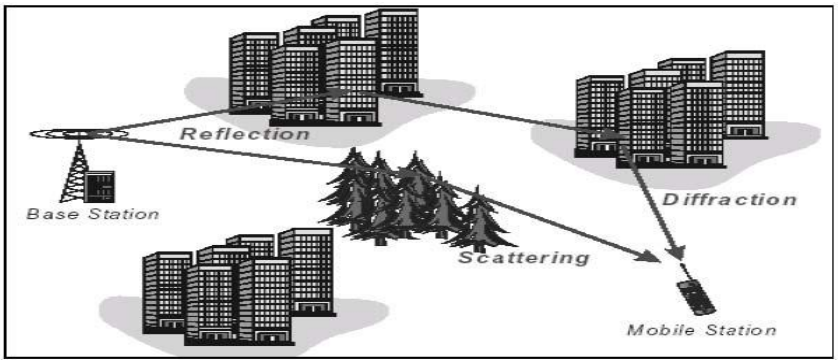

Fig. (1- 1) The three mechanisms in signal propagation in a multipath channel

- **Reflection**

Reflection occurs when a propagating electromagnetic wave encounters a surface that is large relative to the wavelength of the propagating wave [1]. This reflected wave as illustrated in fig (1-2) may interfere constructively or destructively at the receiver due to the change in phase shift after reflection. Sources for reflections include the surface of the earth, buildings and walls.

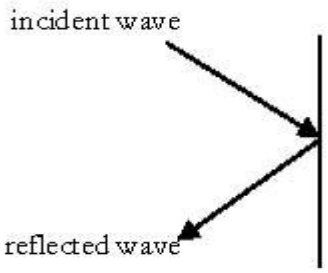

Fig. (1- 2) Reflection of a wave

- **Diffraction**

Fig (1-3) shows that diffraction can occur at the edge of an impenetrable body or at a surface with sharp irregularities that is large compared to the wavelength of the radio wave [3]. The secondary waves resulting from such edges or surfaces are partially reflected and retransmitted with a bend of waves around the obstacle. This allows the signal to be transmitted even when there is no LOS path between the transmitter and the receiver.

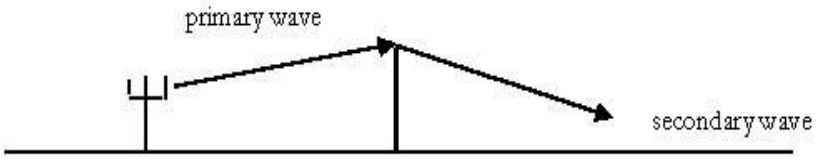

Fig. (1- 3) Diffraction of a wave

- **Scattering**

Scattering occurs when the radio path between the transmitter and receiver consists of large amount of objects with dimensions that are small compared to the wavelength of the signal [1]. Fig (1-4) shows that the scattered waves can be produced by rough surfaces or by other irregularities in the channel such as foliage and traffic signs.

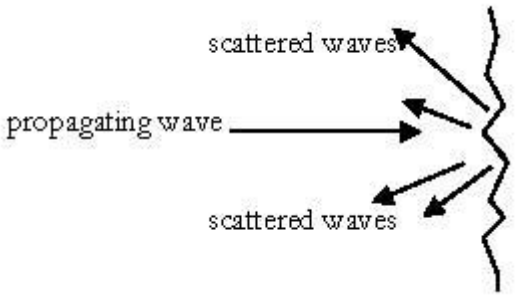

Fig. (1- 4) Scattering of waves

- **Large-scale Fading**

Large-scale fading is primarily attributed to path loss [1] when the received signal strength decays over relatively large distances (several hundreds or thousands of meters) between the transmitter and the receiver as shown in fig (1-5). It is otherwise known as slow fading or shadowing, and is characterized by a long delay spread.

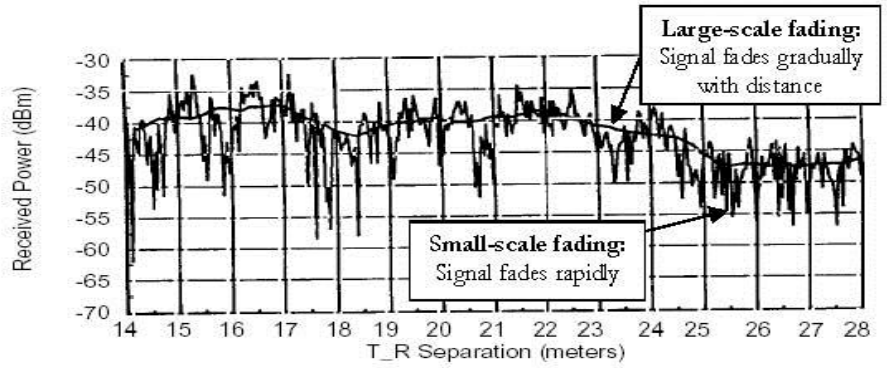

Fig. (1- 5) Large-scale and small-scale fading

- **Small-scale Fading**

Small-scale fading as shown in fig (1-5), manifests itself as rapid fluctuations in the voltage envelope of the received signal over a short period of time or travel distance (a few wavelengths) [1]. It is caused by the interference between two or more versions of the transmitted signal arriving at the receiver with a spread of different times. These time-shifted signals are called multipath signals, which can be represented as ‘taps’ in an impulse-response model of a channel.

Effects of multipath fading can be classified as flat or frequency selective. For flat fading, only the amplitude of the received signal can vary due to the constructive and destructive interference from the time-shifted signals. Frequency selective fading is due to the time dispersion of the received signal and is the cause of inter-symbol interference (ISI).

A tapped-delay line model shown in fig (1-6) demonstrates both the properties of flat and frequency selective fading. Each multipath signal has a different time delay (τ), amplitude level (α) and phase shift (Ø), which will interfere with one another at the receiver, producing a totally distorted version of the original transmitted signal with the addition of noise.

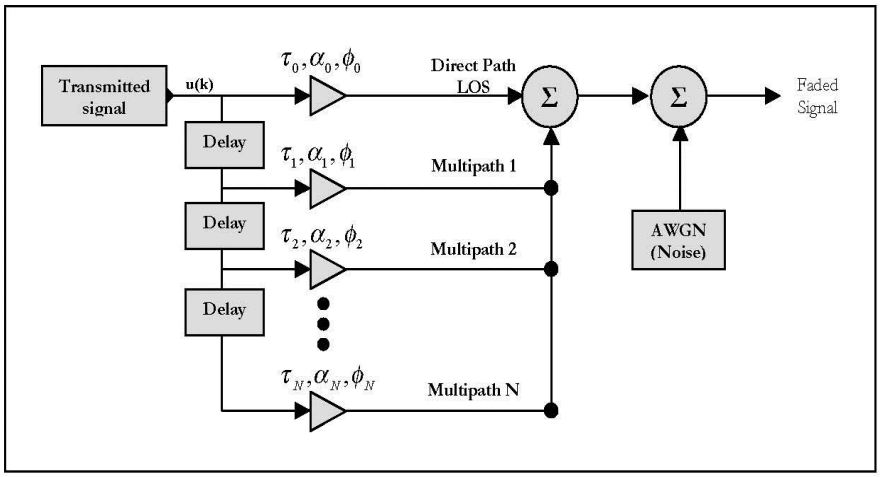

Fig. (1- 6) Tapped delay line model of a multipath fading channel

There are many common models that describe the phenomenon of small scale fading. Out of these models, Rayleigh fading, Rician fading and Nakagami fading models are most widely used. However, for terrestrial path modeling, Additive White Gaussian Noise (AWGN) is commonly used to simulate background noise of the channel under study.

- **Rayleigh fading model**

The Rayleigh fading is primarily caused by multipath reception [4]. Rayleigh fading is a statistical model for the effect of a propagation environment on a radio signal. It is a reasonable model for troposphere and ionospheres' signal propagation as well as the effect of heavily built-up urban environments on radio signals. Rayleigh

fading is most applicable when there is no line of sight between the transmitter and receiver.

- **Rician fading model**

The Rician fading model [4] is similar to the Rayleigh fading model, except that in Ricean fading, a strong dominant component is present. This dominant component is a stationary (non fading) signal and is commonly known as the LOS (Line of Sight Component).

- **AWGN Model**

The simplest radio environment in which a wireless communications system or a local positioning system or proximity detector based on Time of- flight will have to operate is the AWGN [4] environment. AWGN is the commonly used to transmit signal while signals travel from the channel and simulate background noise of channel. The mathematical expression of received signal r(t) = s(t) + n(t) that passed through the AWGN channel where s(t) is transmitted signal and n(t) is background noise.

In wireless radio communication, man-made noise, atmosphere noise, space noise, thermal noise and multipath fading are present and they affect the quality of communications [5]. As a response to these problems RAKE receiver was invented. In this thesis, the performance of RAKE receiver under the conditions of multipath fading will be investigated.

(1-2) Literature Survey

The RAKE receiver is so named because it reminds the function of a garden rake, each finger collecting symbol energy similarly to how tines on a rake collect leaves. The basic idea of a RAKE receiver was first proposed by Price and Green and patented in 1958 (6). It has been studied intensively since then. There are many researches on the design, implementation and simulation of RAKE receiver. We will introduce some of the recent works such as:

A flexible implementation of a WCDMA (Wideband Code Division Multiple Access) Rake receiver is carried out by Lasse Harju et al. [7]. They proposed an ASIC (Application-specific integrated circuit) implementation of a WCDMA Rake receiver targeted for mobile terminals. The implementation is based on a FlexRake architecture that shares hardware resources between multipath components and uses data-level parallelism for despreading multiple code channels. This approach facilitates the flexibility of multipath operation and improves the receiver hardware efficiency. The architecture was implemented using register-transfer-level VHDL (VHSIC Hardware Description Language) description and logic synthesis with standard cells. Synthesis for 0.18 μm CMOS (Complementary metal–oxide–semiconductor) technology resulted in 0.238 mm^2 area and 45.5 μW power consumption at 1.6 V.

Chugh, M. et al. [8] proposed a design and an implementation of configurable W-CDMA Rake receiver architectures on FPGA (field-programmable gate array). They designed and implemented four different architectures for rake receiver on FPGA. These designs are compared for area, frequency and power requirements. A new 'Time Multiplexed Parallel Rake' architecture is proposed, which achieves this objective by two ways. First, it exploits parallelism by processing four chip samples at a time and second, it shares resources for multi code operation by despreading the input samples sequentially in time for each code. The algorithmic correctness of various architectures was first checked by developing a MATLAB model using Simulink blocksets libraries and HDL (Hardware description language) Co-

simulation using Xilinx System Generator. The architectures were implemented on Xilinx Virtex II FPGA family.

A MIMO (multiple-input/multiple-output) RAKE receiver with enhanced interference cancellation is proposed by Jungnickel, V. et al. [9]. They investigated the design of a RAKE receiver for application in the downlink of a wideband code-division multiple access (WCDMA) system in which multiple transmit and multiple receive antennas as well as multiple spreading codes are used. In order to precisely model the space-, code- and intersymbol interference after the RAKE, they derived an equivalent channel model in the space-code domain with two paths corresponding to the current and previous symbol periods. They proposed to cancel all interference jointly with a suitable Wiener filter operating after the RAKE. The filter works fine already with a small number of taps and the receiver performs similar to the well-known chip-level equalizer, provided that both receivers operate over the same time window. An advantage of the RAKE is that the effort scales more directly with the resources used in the space-code domain. On the other hand, short scrambling sequences are needed to enable an efficient implementation of the enhanced interference cancellation.

Doukas, A. et al. [10] presented an implementation of a low complexity Rake receiver and channel estimator for direct sequence spread spectrum (DSSS) systems with main scope to provide adaptability in receiver parameters while keeping the complexity at low levels. The trend in communication systems is towards dynamically adjusting system implementations that can adapt their structure to the continuously changing transmission characteristics. Following this trend they proposed an architecture that is based on the spreading factor of the system, which controls the number of the taps that the CE and the RR will use depending on the current channel conditions. Moreover, based on a resource sharing approach of the main system components, that yet meets the standard bit rates, low complexity is achieved avoiding otherwise necessary complex structures such as complex multipliers. Furthermore they implemented the proposed system on FPGA that gives the ability to

measure performance in terms of bit error rate (BER) in addition to that of power dissipation and area. Thus the performance of the system is compared with the performance of a high level system simulation of the same system, accomplishing the same BER levels. Finally the system implemented on a Xilinx Spartan-3 MB board occupies 56% of the total slices and consumes 103.45 mW with a 5 V supply.

A modified RAKE receiver based on novel Recursive Least Squares (RLS) adaptive algorithm is proposed by Yong Yin et al. [11]. The receiver uses L-fingered correlators, which are composed of RLS adaptive filters, to enhance the performance of multipath receiving. It can also track the amplitude of the received signal to form a real-time amplitude estimation which is correlated with the power of excess delay bin. The simulation results based on the IEEE Ultra Wide Band (UWB) channel models (CM1 to CM4) show that the novel RLS algorithm can alter the attenuation estimation with the finger's power delay profile, and RAKE receiver with few fingers can be employed to get high performance.

Third generation communication systems offer variable spreading factor and multiple codes per user. Hence, the receiver architecture should be configurable to meet varying needs and should consume as little power as possible. To achieve this, different types of RAKE receivers have been designed and implemented. Youssef, M. et al. [12] proposed a new architecture of the RAKE receiver, intended to reduce area consumption and improve scalability. The proposed approach allows for parallel processing of each code on all of the multiple propagation paths on highly regular architecture.

The main feature of ultra wideband (UWB) communication systems is the high resolution of multipath arrivals, which is due to its large transmission bandwidth. Thus, the received signal has many replicas of the transmitted signal, and serious inter-symbol interference (ISI) effects can be made. For direct-sequence ultra wideband (DS-UWB) systems, RAKE receiver despreads the received signal in each finger and combines the despreaded outputs to achieve the multipath

diversity of the desired signal. However, for practice issue, the fingers of RAKE receiver should much less than the number of multipaths. RAKE necessarily optimal. To deal with this problem in such a dense multipath environment, the coefficients of RAKE should be redesigned to maximizing signal energy and suppressing ISI. Ren-Jr Chen & Chang-Lan Tsai [13] designed and analyzed several of receivers based on the RAKE structure, a chip-based equalizer and a novel RAKE/DFE scheme which place a decision-feedback equalizer (DFE) in back of the RAKE receiver to more efficiently cancel the severe ISI. This RAKE/DFE scheme reveals remarkable advantage when low complexity receiver is implemented. Unlike the previous works on with DFE, not just the same as the channel coefficients. Adaptive the RAKE/DFE. The analytical error probability is derived. From simulations, they concluded that the developed RAKE/DFE scheme can suppress can suppress the ISI efficiently.

As another contribution for UWB systems, an N-Selective MRC Rake Receiver with LMS Adaptive Equalizer for UWB Systems is presented by Wan Quan & Anh Dinh [14]. They proposed a receiver to reduce ISI for high speed UWB transmission. The structure consists of an N-selective maximum ratio combiner (MRC) rake receiver and a least-mean-square (LMS) equalizer. This sub-optimal rake receiver processes only a subset of the available resolved multi-path components. A sliding correlation algorithm is used to obtain parameters for the N strongest paths. The LMS equalizer is designed to assist the receiver to reduce ISI. Benefit of this adaptive scheme is the equalizer does not need to know parameters of the entire multi-path component. A short training period with known information sequence is required to initially adjust the tap weights. The equalizer acts as a linear filter to suppress ISI. Simulation results for N=8, 16, and 32 at different values of SNR (Signal-to-noise ratio) show significant improvement in BER. There is only a small trade off in system complexity to obtain such gain.

A Novel Rake Receiver Design for Wideband Wireless Communications is proposed by Konstantinos B. Baltzis & John N.

Sahalos [15]. Its main characteristic is its non-uniform taps distribution. A wide-sense stationary uncorrelated scattering (WSSUS) frequency-selective Rayleigh fading channel is assumed. Uniform and exponential power delay profiles (PDPs) are considered. Taps positions optimization is done according to the Maximum Power Minimum Correlation (MPMC) criterion. This implies the simultaneous maximization of the sum of squares of total average signal power received in each finger and minimization of the sum of squares of autocorrelation between each pair of fingers. Robustness of the technique with respect to errors in channel estimation or in the optimum taps placement is also studied. Several simulation examples of the proposed receiver show its superior performance comparing with other implementations. Finally analytical expressions for the correlation coefficients at the branches outputs of a RAKE receiver for rectangular chip waveforms are derived.

Performance of RAKE receiver in a multipath channel for direct sequence code division multiple access system (DS-CDMA) can be severely impaired due to high level of multiple access interference (MAI), whose value is controlled by correlation functions of user signatures. Due to data modulation MAI becomes dependent on aperiodic user signature correlations of big shifts, which are hard to control and become even less so as multipath delay grows, leading to significant MAI increase. Alexey Dudkov [16] analyzed performance of RAKE receiver for Signature-Interleaved (SI) DS-CDMA in synchronous multipath Rayleigh channel in comparison with that of conventional DS-CDMA. It is shown that SI DS-CDMA provides better performance in terms of bit error rate (BER), especially when using specifically tailored user signatures.

One of the major issues for the design of ultra-wideband (UWB) receivers is the need to recover the signal energy dispersed over many multipath components, while keeping the receiver complexity low. To this aim Cassioli, D et al. [17] considered two schemes for reduced-complexity UWB Rake receivers, both of which combine a subset of the available resolved multipath components. The first method, called partial Rake (PRake), combines theirs/ arriving

multipath components. The second is known as selective Rake (SRake) and combines the instantaneously strongest multipath components. They evaluated and compared the link performance of these Rake receivers in different UWB channels, whose models are based on extensive propagation measurements. They quantified the effect of the channel characteristics on the receiver performance, analyzing in particular the influence of small-scale fading statistics. They found that for dense channels the performance of the simpler PRake receiver is almost as good as that of the SRake receiver, even for a small number of fingers. In sparse channels, however, the SRake outperforms the PRake significantly. They also showed that for a fixed transmitted energy there is an optimum transmission bandwidth.

Recently, multiuser underwater communications become a research area receiving rising attention by both industrials and researchers. (DS/SS) techniques seem to have gained particular attention since it provide improved performance on time varying multipath channels, through the use of coherent-detection based receivers, and allow multiple access communications. Ouertani, K. et al. [18] proposed a performance comparison of two code division multiple access based receivers, a RAKE and a (successive interference cancellation) SIC/RAKE, for an underwater acoustic communication network modems. The developed system is designed for time varying multipath channels in the presence of multiple access interference (MAI), to achieve low probability of intercept (LPI). The performances of the proposed receivers are compared based on computer simulations. Furthermore, Tsimenidis, C.C. et al. [19] concentrated in their work on the design of an adaptive RAKE receiver design for spread-spectrum based communications in shallow water acoustic channels. The objective was to exploit the multipath profile and to combine, rather than cancel, the energy arriving at the receiver via bottom and surface reflections. The optimization of the receiver parameters such as filter weights and phase is achieved by employing the minimum mean-square error (MMSE) criterion. Results indicate that the suggested receiver algorithm can dramatically reduce the number of receive elements

required without any significant performance degradation compared to multichannel combining methods.

Generalized RAKE (G-RAKE) and linear minimum mean square error (LMMSE) are two equalization techniques designed for advanced receivers in WCDMA / high-speed downlink packet access (HSDPA) systems. In [20] Jin He & Salehi, M. first reviewed the theoretical properties and discussed some implementation issues of the G-RAKE technique. The equivalence between G-RAKE and LMMSE chip-level equalization (CE) was then evaluated under various system implementation constraints. Finger placement algorithm is a key factor in implementation and greatly affects the performance of G-RAKE. Optimal solution is prohibitively complex even for small number of fingers since the symbol signal to interference and noise ratio (SINR) is not a convex function of the finger delays. They proposed a novel and computationally efficient finger placement algorithm that significantly reduces the complexity of the optimal solution with a reasonable performance loss. Such algorithm is based on the maximum diagonal weight and therefore named maximum weight placement (MWP). The balance on the performance and the complexity of such algorithm is compared to many proposed algorithms through analysis and simulation results.

In WCDMA systems rake reception is used to combine signal energies of the different multipath components to form a composite signal with better characteristics. A component that is critical to the proper operation of rake receivers is the path searcher. The searcher estimates the delays of the multipath component where each delay corresponds to a separate multipath component. Sagahyroon, A. et al. [21] presented an FPGA implementation of the path searcher. Details of the implementation and experimental results are discussed. FPGA computational output is verified using MATLAB based simulation.

Chaitanya, K.S. et al. [22] presented a system-on-chip (SoC) solution for RAKE receiver using a CORDIC (Coordinate Rotation Digital Computer) hardware accelerator. The algorithm is implemented on Cyclone II FPGA device chipped on Altera DE2 board. The inbuilt

NIOS II soft core processor of the FPGA device acts as the processor for processing applications. The CORDIC algorithm which computes the trigonometric functions is developed as a custom instruction for the NIOS II processor. This hardware accelerator has drastically improved the performance of the algorithm by about 70% when compared with the pure software implementation. This improvement in the performance is achieved at the cost of area. The performance of RAKE receiver is illustrated using bit error rate (BER) calculations. The RAKE receiver performance is examined and compared using maximal ratio and equal-gain combining techniques.

A low-complexity architecture of a RAKE Receiver subsystem for a Direct Sequence Ultra-Wideband (DS-UWB) is presented by Thomos, C. & Kalivas, G. [23], followed by FPGA implementation and system performance results. The proposed subsystem is composed of a Channel Estimator (CE) and a novel hybrid Partial/Selective (HPS) maximal ratio combining (MRC) RAKE Receiver, which combines the benefits of both partial and selective RAKE receiver algorithms. The implementation of the HPS component is based on a parallel selection structure that picks the strongest multipath rays of the channel impulse response. Their work is focused on a highly parallel, modular design based on FPGA technology and optimized for high performance. The obtained results demonstrate the tradeoff between energy capture, performance and receiver complexity.

For multiple access high data rate UWB systems, ISI and MAI will influence the performance of the systems. In [24], a Rake receiver structure is presented by Lina Qi et al., with adjusting the tap weights adaptively using RLS algorithm, in which the optimal parameters of RLS algorithm can be determined by part of the channel state information(CSI). Simulation results show that the proposed receiver based on RLS algorithm performs close to the infinite Rake receiver bound limit, and the system with it can achieve good performance under proper parameters of the RLS.

A new model of Multi-Carrier Code Division Multiple Access (MC-CDMA) RAKE receiver has been proposed by Choudhury, S.H. et al. [25] for multipath fading mitigation based on maximum ratio combining diversity. The analytical model has been verified considering Rayleigh multipath fading channel. The simulation results substantiate that the proposed MC-CDMA RAKE receiver provides better immunity to multipath fading and offers improved BER performance than conventional MC-CDMA receiver.

Many different types of RAKE receiver have been appeared with the development of mobile telecommunication. It is necessary to evaluate their application value. In the work done by Haiyang Fu et al. [26], the models of DIRAKE, CORAKE and CLRAKE receiver and their specific implementations are put forward. Moreover, their performances are also discussed when MPI and MAI exist. According to the results of performance simulation, it can be found that CORAKE receiver has better performance than CLRAKE receiver, and is easier to be realized. When the beam is formed in baseband, the performance of DIRAKE receiver is influenced greatly by the change of MS's position, which will introduce instability into the system.

(1-3) Organization of the thesis

This thesis report consists of five chapters in total. The framework for the thesis is described as follows:

The introductory chapter provides a brief introduction about signal propagation characteristics in a wireless radio channel and how the resultant waveform at the receiver can be severely distorted and the need for using RAKE receiver, and a literature survey about previous work.

Chapter 2 explains the basic concept and principles of spread spectrum technology, different types of spreading codes and their properties, and principle of direct sequence spread spectrum modulation.

Chapter 3 contains the concept and different types of diversity, different combining techniques and their performance, principle and functionality of the RAKE receiver, and the principle of the LMS algorithm and its role in channel delay estimation.

Chapter 4 presents the simulation hierarchy of our work including detailed matlab models, simulation results, and bit error rate comparisons.

Finally, chapter 5 gives the reader an overall summary on the collated results. This chapter concludes with recommendations and improvements for any future research work in this topic.

Chapter 2: Spread - Spectrum Modulation

(2-1) Introduction

The spread spectrum modulation techniques are originally developed for use in the military and intelligence communications systems due to their resistance against jamming signals and low probability of interception (LPI) [27]. They are immune to various kinds of noise and multipath distortion. Apart from these advantages, spread spectrum signals also have the capability to support multiple users at the same time by assigning each user with an orthogonal spreading code. For the sake of secure communications, channel bandwidth and transmit power are sacrificed [28].

Literally, a spread spectrum system is one in which the transmitted signal is spread over a wide frequency band, much wider than the minimum bandwidth required to transmit the information being sent [29] see Fig. (2-1).

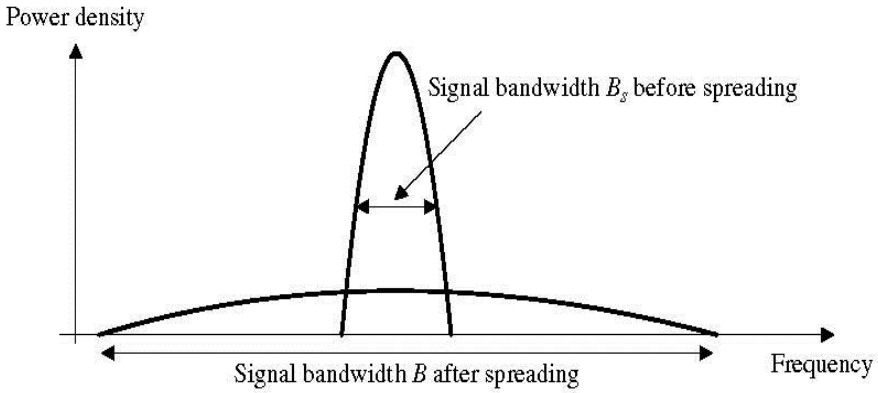

Fig. (2- 1) Power spectral density before and after spreading

(2-2) Theoretical Justification for Spread Spectrum

The principle behind the spreading of a signal is explained by the Shannon channel capacity formula:

$$C = B \log_2 \left(1 + \frac{S}{N}\right) \quad (2.1)$$

Where C is the capacity of a communication channel in bits per sec, B is the bandwidth in hertz, S is the signal power, and N is the noise power. Equation (2.1) can be rewritten as

$$\frac{C}{B} = 1.44 \ln \left(1 + \frac{S}{N}\right) \quad (2.2)$$

Which at small SNRs can be approximated as follows:

$$\frac{C}{B} = 1.44 \frac{S}{N} \quad (2.3)$$

or

$$B \simeq \frac{NC}{s} \quad (2.4)$$

From equation (2.4) the necessary bandwidth for error-free transmission information at very low SNR can be calculated. It demonstrates that as the relative noise level increases, reliable transmission is possible by increasing bandwidth [30, 31].

(2-3) Advantages of spread spectrum

1. **Resistance to Interference and Antijamming Effects**: There are many benefits to spread-spectrum technology. Resistance to interference is the most important advantage. Intentional or unintentional interference and jamming signals are rejected because they do not contain the spread-spectrum key. Only the desired signal, which has the key, will be seen at the receiver when despreading is performed [32].

2. **Resistance to Interception**: Resistance to interception is the second advantage provided by spread-spectrum techniques. Because nonauthorized listeners do not have the key used to spread the original signal, those listeners cannot decode it. Without the right key, the spread-spectrum signal appears as noise or as an interferer. Even better, signal levels can be below the noise floor, because the spreading operation reduces the spectral density. Other receivers cannot "see" the transmission; they only register a slight increase in the overall noise level.

3. **Multiple access capability:** That rejection also applies to other spread-spectrum signals that do not have the right key. Thus different spread-spectrum communications can be active simultaneously in the same band, such as CDMA, allowing multiple access capability.

4. **Resistance to Fading (Multipath Effects):** Wireless channels often include multiple-path propagation in which the signal has more than one path from the transmitter to the receiver (Fig. (2-2)). Such multipath can be caused by atmospheric reflection or refraction and by reflection from the ground or from objects such as buildings as explained before. The reflected path (R) can interfere with the direct path (D) in a phenomenon called fading. Because the despreading process synchronizes to signal D, signal R is rejected even though it contains the same key. Methods are available to use the reflected-path signals by despreading them and adding the extracted results to the main one.

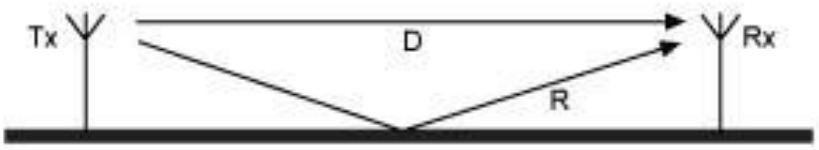

Fig. (2- 2) Illustration of how the signal can reach the receiver over multiple paths.

5. **Longer operating distances:** A spread spectrum device operated in the industrial, scientific and medical (ISM) band is allowed to have higher transmitted power due to its non-interferencing nature. Because of the higher transmit power; the operating distance of such a device can be significantly longer than that of a traditional analog wireless communication device [33].

A number of modulation techniques have been developed to generate spread spectrum signals. These can be generally classified as direct-sequence spread spectrum (DS-SS), frequency-hopping spread spectrum (FH-SS), time-hopping spread spectrum (TH-SS), chirp modulation and the hybrid combination modulation [27]. In this chapter, we discuss principles of spread-spectrum modulation, with emphasis on direct-sequence. In a DSSS technique, two stages of modulation are used. First, the incoming data sequence is used to modulate a wide band code. This code transforms the narrowband data sequence into a noiselike wideband signal. For its operation, this technique relies on the availability of a noiselike spreading code called a pseudo-random or pseudo-noise sequence.

(2-4) Pseudo-Noise Sequences

A pseudo-noise (PN) sequence is a periodic binary sequence with a noiselike waveform that is usually generated by means of a feedback shift register, a general block diagram of which is shown in Fig. (2-3). A feedback shift register consists of an ordinary shift register made up of m flip-flops and a logic circuit that are interconnected to

form a multiloop feedback circuit. With a total number of m flip-flops, the number of possible states of the shift register is at most 2^m-1. It follows therefore that the PN sequence generated by a feedback shift register must eventually become periodic with a period of at most 2^m [28].

So we can say that *PN* sequences are:

- Not random, but it looks randomly for the user who doesn't know the code.

- Deterministic, periodical signal that is known to both the transmitter and the receiver. The longer the period of the PN spreading code, the closer will the transmitted signal be a truly random binary wave, and the harder it is to detect.

- Statistical properties of sampled white-noise [34].

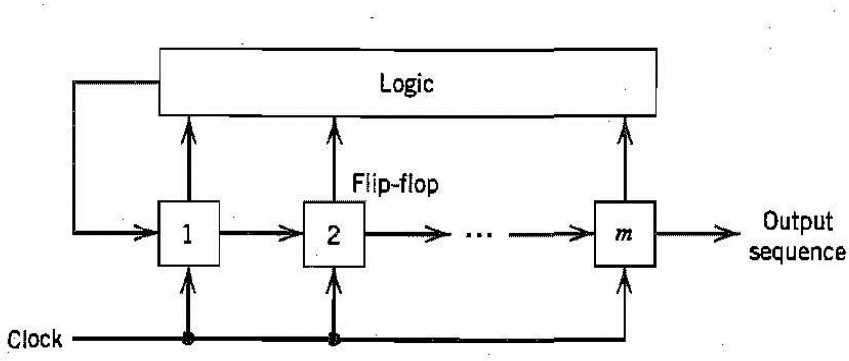

Fig. (2- 3) Feedback shift register with *m* stages

(2-4-1) Properties of random Sequences

1. *Balance Property*: In each period of the sequence the number of binary ones differs from the number of binary zeros by at most one digit (for N odd).When modulating a carrier with a PN coding sequence, one-zero balance (DC component) can limit the degree of carrier suppression obtainable, because

carrier suppression is dependent on the symmetry of the modulating signal.

2. *Run-length Distribution:* A run is a sequence of a single type of binary digits. Among the runs of ones and zeros in each period it is desirable that about one-half the runs of each type are of length 1, about one-fourth are of length 2, one-eigth are of length 3, and so on.

3. *Autocorrelation:* The origin of the name pseudo-noise is that the digital signal has an autocorrelation function which is very similar to that of a white noise signal: impulse like. The autocorrelation function for the periodic sequence pn is defined as the number of agreements less the number of disagreements in a term by term comparison of one full period of the sequence with a cyclic shift (position t) of the sequence itself:

$$R_a(\tau) = \frac{1}{T_b} \int_{-T_b/2}^{T_b/2} c(t)c(t-\tau)\ dt \qquad (2.5)$$

Where $R_a(\tau)$ is the autocorrelation function of a periodic signal $c(t)$ of period T_b .

For PN sequences the autocorrelation has a large peaked maximum (only) for perfect synchronization of two identical sequences (like white noise). The synchronization of the receiver is based on this property.

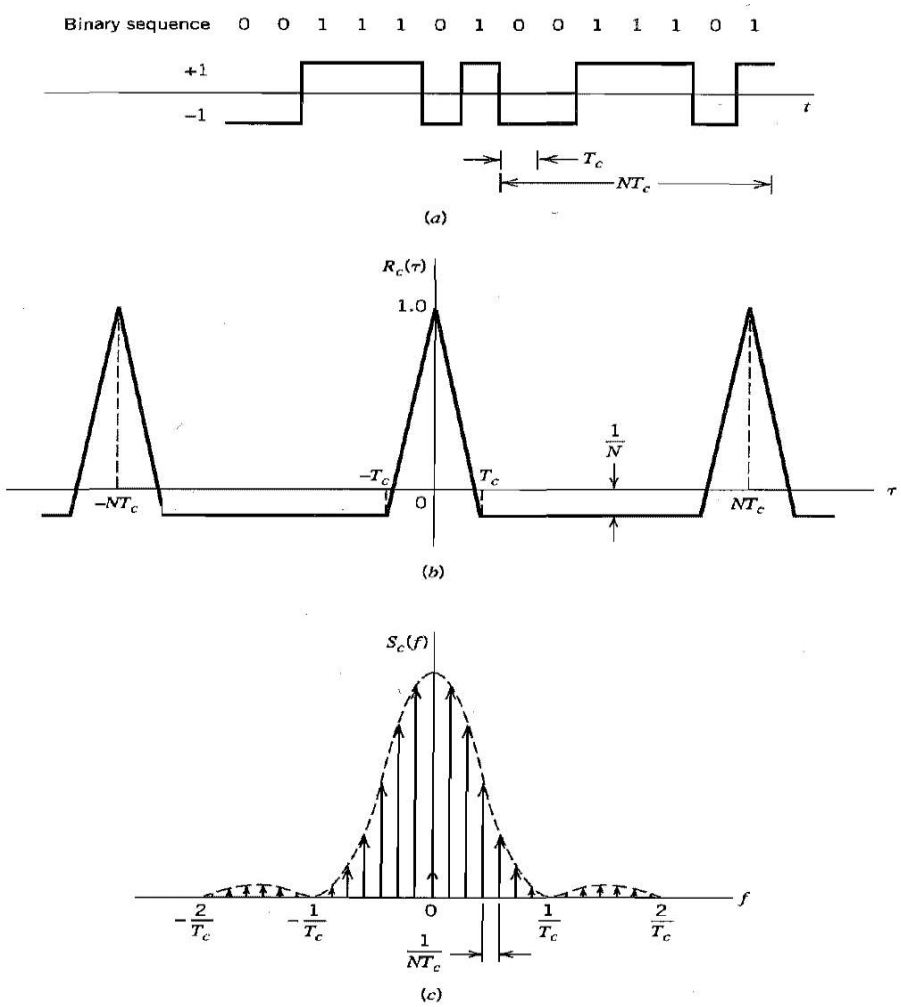

Fig. (2- 4) *(a)* Waveform of PN sequence for length m = 3 or period N = 7. *(b)* Autocorrelation function. *(c)* Power spectral density.

4. *Frequency Spectrum*: Due to the periodic nature of the PN seqeunce the frequency spectrum has spectral lines which become closer to each other with increasing sequence length N. Each line is further smeared by data scrambling, which spreads each spectral line and further fills in between the lines to make the spectrum more nearly continuous. The DC component is determined by the zero-one balance of the PN sequence [34]. Fig. (2-4) shows the waveform of PN sequence

of length m=3 with a plot of its autocorrelation function and power spectral density.

5. *Cross-correlation*: Cross-correlation describes the interference between codes i and j :

$$R_c(\tau) = \frac{1}{T_b} \int_{-T_b/2}^{T_b/2} c_i(t) c_j(t-\tau)\ dt \qquad (2.6)$$

If the cross-correlation $R_c(\tau)$ is zero for all t, the codes are called *orthogonal*. In CDMA multiple users occupy the same RF bandwidth and transmit simultaneous. When the user codes are orthogonal, there is no interference between the users after despreading and the privacy of the communication of each user is protected. In practice, the codes are not perfectly orthogonal; hence the cross-correlation between user codes introduces performance degradation (increased noise power after despreading), which limits the maximum number of simultaneous users.

(2-4-2) Types of PN sequences

1- m-sequence

A Simple Shift Register Generator (SSRG) has all the feedback signals returned to a single input of a shift register (delay line) [34]. The SSRG is linear if the feedback function can be expressed as a modulo-2 sum (xor).

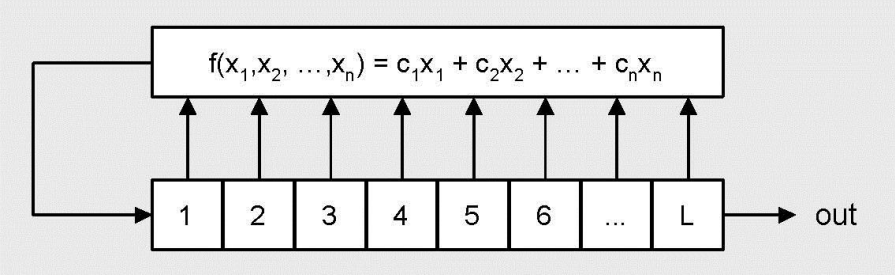

Fig. (2- 5) A Simple Shift Register Generator (SSRG)

The feedback function f($x_1, x_2, \ldots, x_n$) is a modulo-2 sum of the contents $x_i$of the shift register cells with c_i being the feedback connection coefficients (c_i=0=open, c_i=1=connect). An SSRG with L flip- flops produces sequences that depend upon register length L, feedback tap connections and initial conditions. When the period (length) of the sequence is exactly N_c= 2^L -1, the PN sequence is called a *maximum-length sequence* or simply an *m-sequence*. An m-sequence generated from a linear SSRG has an *even number of taps*. If an L-stage SSRG has feedback taps on stages L, k, m and has sequence … , a_i, a_{i+1}, a_{i+2},… than the *reverse SSRG* has feedback taps on L, L-k, L-m and sequence … , a_{i+2}, a_{i+1}, a_i, … .

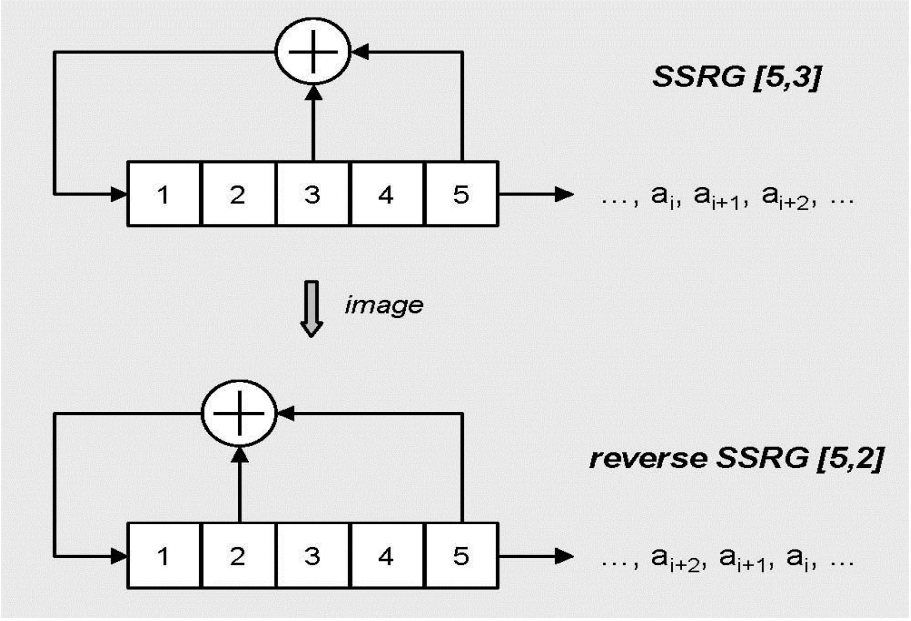

Fig. (2- 6) An example of m-sequence generator

In the following table the feedback connections (even number) are tabulated for m-sequences generated with a linear SSRG (without image set). For every set feedback taps listed in the table, there exists an image set (reverse set) of feedback taps that generates an identical sequence reversed in time.

Table (2- 1) Table for feedback connections of m-sequence

L	$N_c=2^L-1$	Feedback Taps for m-sequences	# m-sequences
2	3	[2,1]	2
3	7	[3,1]	2
4	15	[4,1]	2
5	31	[5,3] [5,4,3,2] [5,4,2,1]	6
6	63	[6,1] [6,5,2,1] [6,5,3,2]	6
7	127	[7,1] [7,3] [7,3,2,1] [7,4,3,2] [7,6,4,2] [7,6,3,1] [7,6,5,2] [7,6,5,4,2,1] [7,5,4,3,2,1]	18
8	255	[8,4,3,2] [8,6,5,3] [8,6,5,2] [8,5,3,1] [8,6,5,1] [8,7,6,1] [8,7,6,5,2,1] [8,6,4,3,2,1]	16
9	511	[9,4] [9,6,4,3] [9,8,5,4] [9,8,4,1] [9,5,3,2] [9,8,6,5] [9,8,7,2] [9,6,5,4,2,1] [9,7,6,4,3,1] [9,8,7,6,5,3]	48
10	1023	[10,3] [10,8,3,2] [10,4,3,1] [10,8,5,1] [10,8,5,4] [10,9,4,1] [10,8,4,3] [10,5,3,2] [10,5,2,1] [10,9,4,2] [10,6,5,3,2,1] [10,9,8,6,3,2] [10,9,7,6,4,1] [10,7,6,4,2,1] [10,9,8,7,6,5,4,3] [10,8,7,6,5,4,3,1]	60
11	2047	[11,2] [11,8,5,2] [11,7,3,2] [11,5,3,2] [11,10,3,2] [11,6,5,1] [11,5,3,1] [11,9,4,1,] [11,8,6,2,] [11,9,8,3] [11,10,9,8,3,1]	176

- **Properties of m-sequences**

M-sequences have many of the properties possessed by a truly random binary sequence. Some properties of maximal-length sequences are as follows [28]:

1. *Balance property*: In each period of a maximal-length sequence, the number of 1s is always One more than the number of 0s.
2. *Run property*: Among the runs of 1s and of 0s in each period of a maximal-length sequence, one-half the runs of each kind

are of length one, one-fourth are of length two, one-eighth are of length three, and so on. For a maximal-length sequence generated by a linear feedback shift register of length *l*, the total number of runs is (N + 1)/2, where $N = 2^l - 1$.

3. *Correlation property*: The autocorrelation function of a maximal-length sequence is periodic and binary valued. The autocorrelation function of the m-sequence is –1 for all values of the chip phase shift τ, except for the [-1, +1] chip phase shift area, in which correlation varies linearly from the -1 value to $2^l - 1 = N$ (the sequence length). This is shown in fig. (2-7).

The autocorrelation peak increases with increasing length N of the m-sequence and approximates the autocorrelation function of white noise [34]. Other codes can do no better than equal this performance of m-sequences.

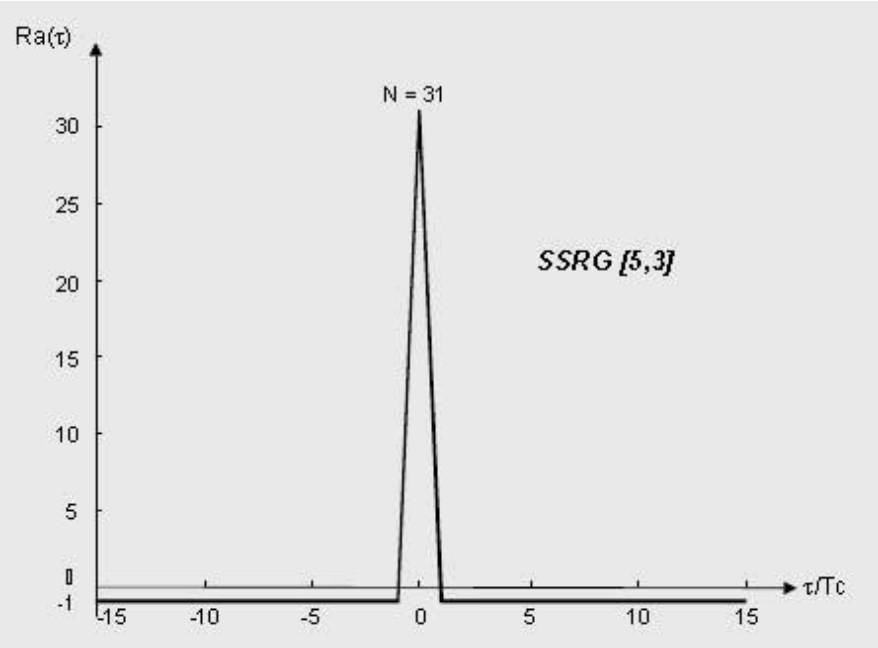

Fig. (2- 7) Autocorrelation function of m- sequence for length *l* = 5 or period N = 31.

4. *Crosscorrelation*: Cross-correlation is the measure of agreement between two different codes. Unfortunately, crosscorrelation is not so well behaved as autocorrelation. In multi-user environment, the code sequences must be carefully chosen to avoid interference between users.
5. *Security*: The m-sequence codes are linear, and thus not usable to secure a transmission system. The linear codes are easily decipherable once a short sequential set of chips ($2l$+1) from the sequence is known. The overall system could still be secure if the information itself where encoded by a cryptographically secure technique.

2- Barker Codes

The Barker code gives codes with different lengths and very similar autocorrelation properties as the m-sequences. The table below lists all known Barker codes [35], however only codes of length 11 and 13 are used in DS-SS.

Table (2- 2) Existing Barker code.

Code Length	Coded signal
2	10, 11
3	110
4	1101,1110
5	11101
7	1110010
11	11100010010
13	1111100110101

3- Gold Codes

The autocorrelation properties of the m-sequences cannot be bettered. But a multi-user environment needs a set of codes with the same

length and with good cross-correlation properties. Gold code sequences are useful because a large number of codes (with the same length and with controlled crosscorrelation) can be generated, although they require only one 'pair' of feedback tap sets [34].

A set of *N* Gold sequences is derived from a preferred pair of *m*-sequences of length $2^l - 1$ by taking the modulo-2 sum of the first preferred *m*-sequence with the cyclically shifted versions of the second preferred *m*-sequence. By including the two preferred *m*-sequences, a family of 2^l +1 Gold codes is obtained. Gold codes have a three-valued cross correlation function with values {−1,−*t (l), t (l)* − 2} where

$$\mathrm{t}(l) = \begin{cases} 1 + 2^{(l+1)/2} & \text{for } l \text{ odd} \\ 1 + 2^{(l+2)/2} & \text{for } l \text{ even} \end{cases} \qquad (2.7)$$

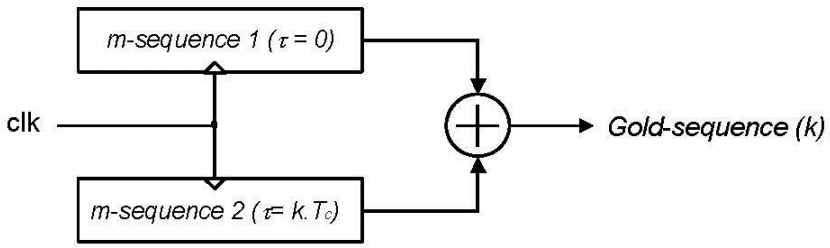

Fig. (2- 8) Generation of Gold sequence

Thus, in order to generate a family of Gold codes, it is necessary to find a preferred pair of *m*-sequences. The following conditions are sufficient to define a preferred pair, **b** and **b'**, of *m*-sequences [36]:

1. $l \neq 0 \bmod 4$; that is, *l* is odd or $l = 2 \bmod 4$.
2. **b'** = **b** [*q*] ,where *q* is odd and either

$$q = 2^k+1 \tag{2.8}$$

or

$$q = 2^{2k} - 2^k + 1 \tag{2.9}$$

Where **b** [q] is the qth decimation of **b**.

3. $$\gcd(l,k) = \begin{cases} 1, & \text{for } l \text{ odd} \\ 2, & \text{for } l = 2 \bmod 4 \end{cases} \tag{2.10}$$

In Item 2 above, **b**' = **b** [q] is known as a *proper* decimation of **b** which is obtained by sampling every qth symbol of **b** and obtaining another *m*-sequence (which may not always be the case, thus giving an *improper* decimation).

Table (2- 3) Subset of Gold codes with the corresponding Preferred Pairs of m-sequence

L	$\boldsymbol{N = 2^l - 1}$	Preferred pairs of m-sequence	3-value crosscorrelations		
5	31	[5,3] [5,4,3,2]	7	-1	-9
6	63	[6,1] [6,5,2,1]	15	-1	-17
7	127	[7,3] [7,3,2,1] [7,3,2,1] [7,5,4,3,2,1]	15	-1	-17
8*	225	[8,7,6,5,2,1] [8,7,6,1]	31	-1	-17
9	511	[9,4] [9,6,4,3] [9,6,4,3] [9,8,4,1]	31	-1	-33
10	1023	[10,9,8,7,6,5,4,3] [10,9,7,6,4,1] [10,8,7,6,5,4,3,1] [10,9,7,6,4,1] [10,8,5,1] [10,7,6,4,2,1]	63	-1	-65
11	2047	[11,2] [11,8,5,2] [11,8,5,2] [11,10,3,2]	63	-1	-65

(2-5) Orthogonal Codes

Two sequences are said to be orthogonal when the inner product between the two sequences is zero. If $c_i(k\tau)$ and c_j $(k\tau)$ are the *ith* and *jth* orthogonal members of an orthogonal set, respectively, *M* is the length of the set and τ is the symbol duration, then the orthogonal property states that

$$\sum_{k=0}^{M-1} c_i(k\tau)c_j(k\tau) = 0 \qquad i \neq j \tag{2.11}$$

Different PN as well as orthogonal sequences can be used as spreading codes for CDMA cellular networks or can be used for encrypting speech signals to reduce the residual intelligence. More details about both kinds of sequence can be found in [37]. The main type of orthogonal codes is Walsh-Hadamard codes.

(2-5-1) Walsh-Hadamard codes

Walsh-sequences have the advantage to be orthogonal, in this way we should get rid of any multi-access interference under a perfect synchronization [38]. In particular, the Walsh-Hadamard codes of length N can be defined from the following recurrent rule (the same as the Walsh-Hadamard transform):

$$H_0 = [1];$$

$$H_1 = \begin{bmatrix} H_0 & H_0 \\ H_0 & -H_0 \end{bmatrix};$$

$$H_{i+1} = \begin{bmatrix} H_i & H_i \\ H_i & -H_i \end{bmatrix}; \qquad \text{i} = 1,\ldots..,\ log_2(\text{N}) - 1; \tag{2.12}$$

There are however a number of drawbacks:

- The codes do not have a single, narrow autocorrelation peak.
- The spreading is not over the whole bandwidth, instead the energy is spread over a number of discrete frequency-components.

- Although the full-sequence cross-correlation is identically zero, this does not hold for partial sequence cross-correlation function. The consequence is that the advantage of using orthogonal codes is lost.
- Orthogonality is also affected by channel properties like multi-path. In practical systems equalization is applied to recover the original signal.

These drawbacks make Walsh-sequences not suitable for non-cellular systems. Systems in which Walsh-sequences are applied are for instance multi-carrier CDMA and the cellular CDMA system IS-95 (Interim Standard 95). Both systems are based on a cellular concept; all users (and so all interferers) are synchronized with each other.

(2-6) Direct-Sequence Spread Spectrum (DS-SS)

The DS-SS technique is one of the most popular forms of spread spectrum. This is probably due to the simplicity with which direct sequencing can be implemented. The general principle behind DS-SS is that the information signal with bandwidth *Bs* is spread over a bandwidth *B*, where *B* >> *Bs* [29]. The processing gain is specified as

$$P_G = \frac{B}{B_s} \tag{2.13}$$

The higher the processing gain, the lower the power density one needs to transmit the information. If the bandwidth is very large, the signal can be transmitted such that it appears like a noise.

One method of widening the bandwidth of a data sequence involves the use of modulation. Let the waveforms b(t) denote the data signal and c(t) denote the the PN signal. The desired modulation is achieved by applying the data signal b(t) and the PN signal c(t) to a product modulator or multiplier, as in Fig. (2-9-a). From Fourier transform theory; multiplication of two signals produces a signal whose spectrum equals the convolution of the spectra of the two component signals. Thus, if the message signal b(t) is narrowband and the PN signal c(t) is wideband, the product (modulated) signal m(t) will have

a spectrum that is nearly the same as the wideband PN signal. In other words, the PN sequence performs the role of a spreading code.

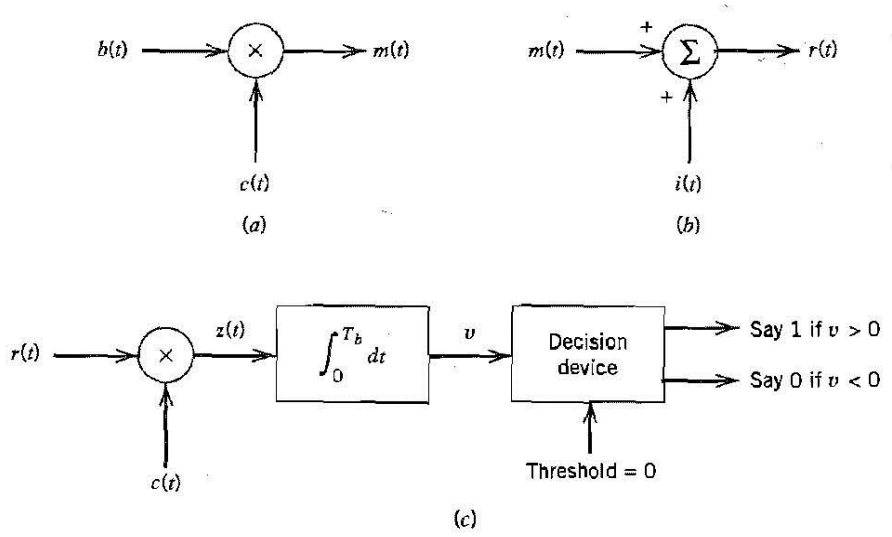

Fig. (2- 9) Idealized model of baseband spread-spectrum system. *(a)* Transmitter. *(b)* Channel. *(c)* Receiver.

By multiplying the information-bearing signal *b(t)* by the PN signal *c(t)*, each information bit is "chopped" up into a number of small time increments called *chips*, as illustrated in the waveforms of Fig. (2-10). For *baseband* transmission, the product signal *m(t)* represents the *transmitted signal.* We may thus express the transmitted signal as

$$m(t) = c(t)b(t) \tag{2.14}$$

The received signal *r(t)* consists of the transmitted signal *m(t)* plus an additive *interference* denoted by *i(t)*, as shown in the channel model of Fig. (2-10-b). Hence,

$$\begin{aligned} r(t) &= m(t) + i(t) \\ &= c(t)b(t) + i(t) \end{aligned} \tag{2.15}$$

To recover the original message signal *b(t)*, the received signal *r(t)* is applied to a *demodulator* that consists of a multiplier followed by an

integrator, and a decision device, as in Figure *2.9c*. The multiplier is supplied with a locally generated PN sequence that is an exact *replica* of that used in the transmitter. Moreover, we assume that the receiver operates in perfect *synchronism* with the transmitter. The multiplier output in the receiver is therefore given by

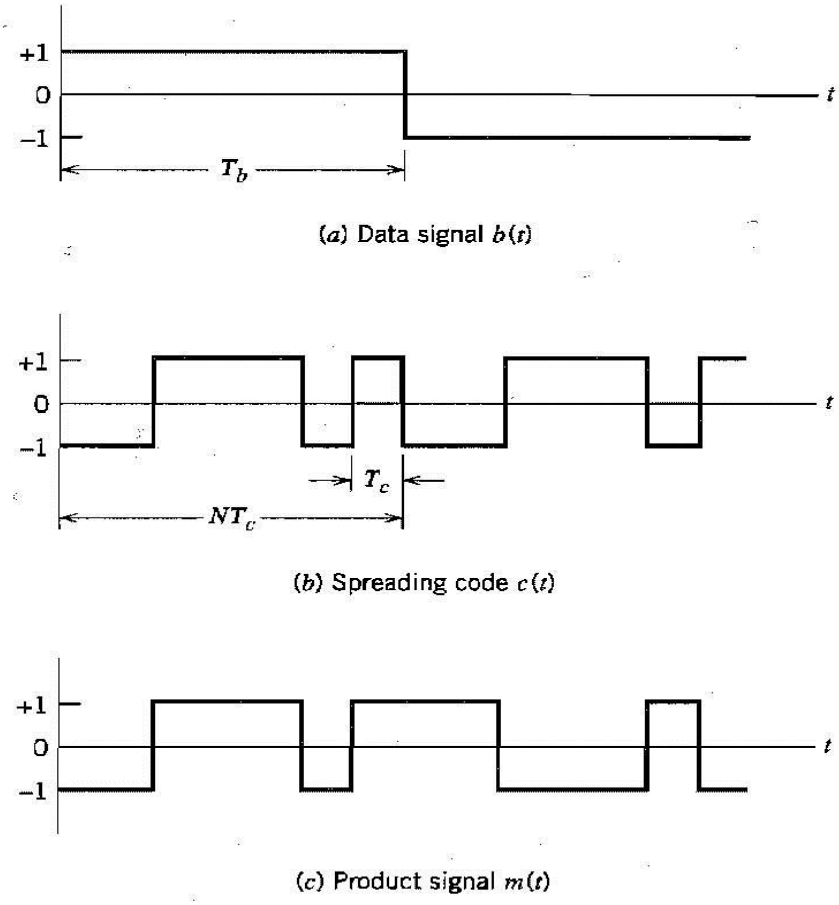

Fig. (2- 10) Illustrating the waveforms in the transmitter of fig. (2-9)

$$z(t) = c(t)r(t)$$

$$= c^2(t)b(t) + c(t)i(t) \qquad (2.16)$$

Since

$$c^2(t) = 1\,, \qquad \text{for all t} \qquad (2.17)$$

Accordingly, we may simplify Equation (2.16) as

$$z(t) = b(t) + c(t)\,i(t) \qquad (2.18)$$

We thus see from Equation (2.18) that the data signal b(t) is reproduced at the multiplier output in the receiver, except for the effect of the interference represented by the additive term c(t)i(t). We now observe that the data component b(t) is narrowband, Whereas the spurious component c(t)i(t) is wideband. Hence, by applying the multiplier output to a baseband (low-pass) filter with a bandwidth just large enough to accommodate the recovery of the data signal b(t), most of the power in the spurious component c(t)i(t) is filtered out as shown in Fig. (2-11) [39].

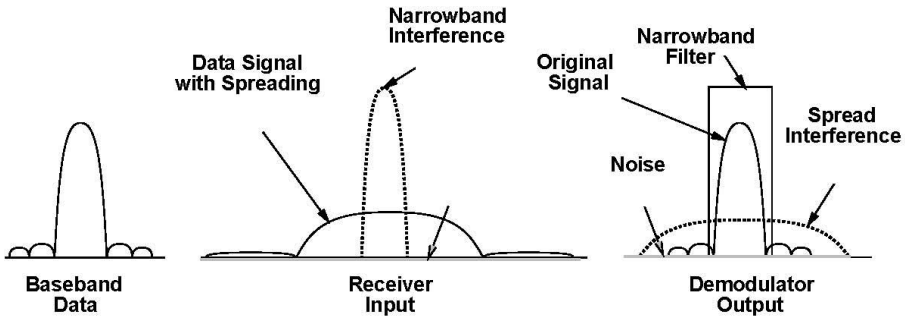

(a) (b) (C)

Fig. (2- 11) Signal and Interference a)before spreading b) after spreading c)after despreading

In the receiver shown in Fig. (2-11-c), the low-pass filtering action is actually performed by the integrator that evaluates the area under the signal produced at the multiplier output. The integration is carried out

for the bit interval $0 \leq t \leq T_b$, providing the sample value *v*. Finally, a decision is made by the receiver: If *v* is greater than the threshold of zero, the receiver says that binary symbol 1 of the original data sequence was sent, and if v is less than zero, the receiver says that symbol 0 was sent.

(2-6-1) DS-SS with Coherent Binary Phase-Shift Keying

The spread-spectrum technique described in the previous section is referred to as direct sequence spread spectrum for baseband transmission. To use this technique in passband transmission over a satellite channel, for example, coherent *binary phase-shift keying* (PSK) may be used in the transmitter and receiver, as shown in Fig. (2-12). The transmitter of Fig. (2-12-a) first converts the incoming binary data sequence $\{b_k\}$ into a polar non-return-to-zero (NRZ) waveform *b(t)*, which is followed by two stages of modulation. The first stage consists of a product modulator or multiplier with the data signal *b(t)* and the PN signal *c(t)* as inputs. The second stage consists of a binary PSK modulator. The transmitted signal *x(t)* is thus a *direct-sequence binary phase-shift-keyed (DS/BPSK) signal.* The phase modulation $\vartheta(t)$ of *x(t)* has one of two values, 0 and π, depending on the polarities of the message signal *b(t)* and PN signal *c(t)* at time *t.*

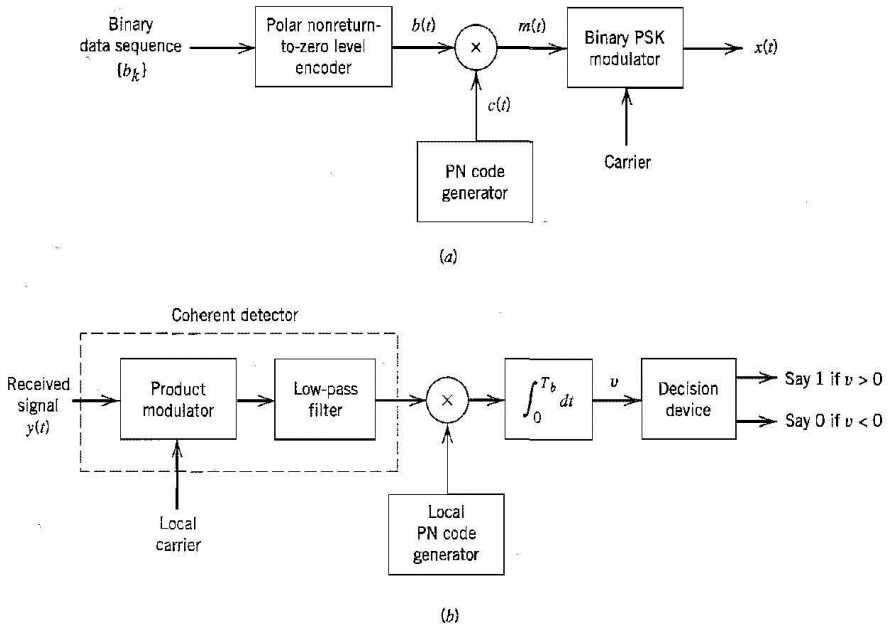

Fig. (2- 12) Direct-sequence spread coherent phase-shift keying. *(a)* Transmitter. *(b)* Receiver.

Fig. (2-13) illustrates the waveforms for the second stage of modulation. The waveform shown here corresponds to one period of the PN sequence. Fig. (2-13-b) shows the waveform of a sinusoidal carrier, and Fig. (2-13-c) shows the *DS/BPSK* waveform that results from the second stage of modulation.

The receiver shown in Fig. (2-12-b), consists of two stages of demodulation. In the first stage, the received signal *y(t)* and a locally generated carrier are applied to a product modulator followed by a low-pass filter whose bandwidth is equal to that of the original message signal *m(t).* This stage of the demodulation process reverses the phase-shift keying applied to the transmitted signal. The second stage of demodulation performs spectrum despreading by multiplying the low-pass filter output by a locally generated replica of the PN signal *c(t),* followed by integration over a bit interval $0 \leq t \leq T_b$, and finally decision making in the manner described in previous sec.

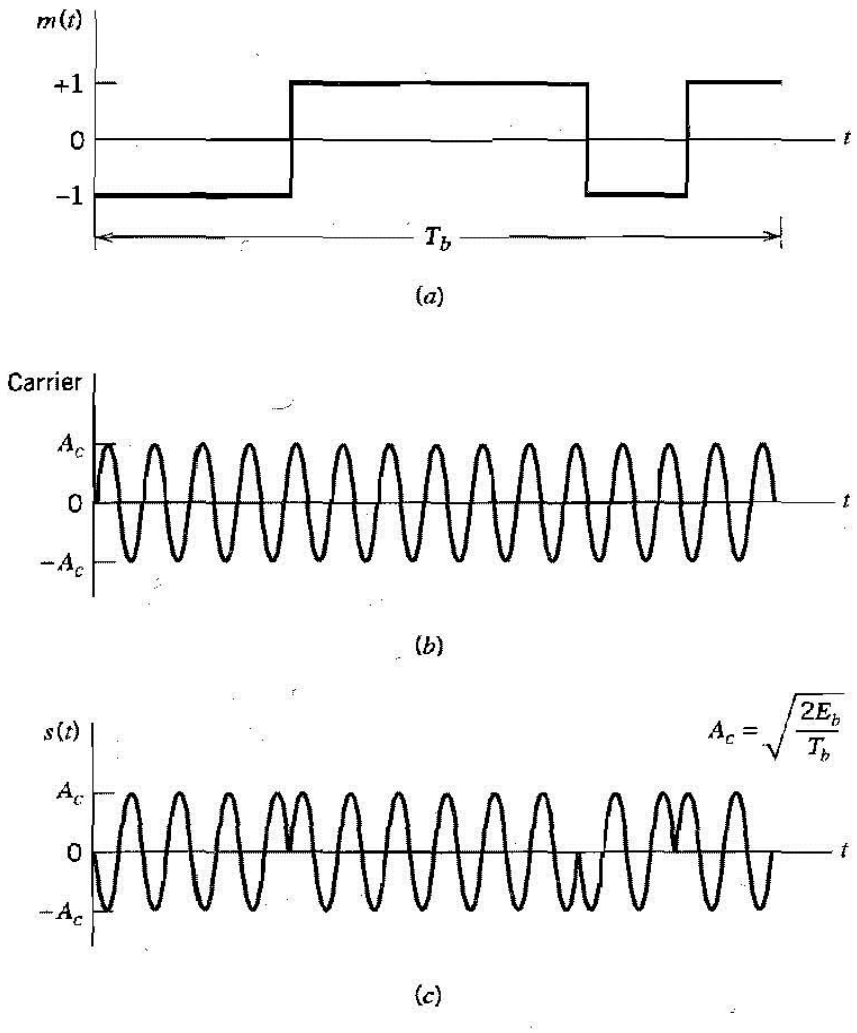

Fig. (2- 13) *(a)* Product signal *m(t) = c(t)b(t). (b)* Sinusoidal carrier. *(c)* DS/BPSK signal.

(2-6-2) Advantages and Drawbacks of DS in multiuser environment

Conventional DS-SS systems offer several advantages in cellular environments including easy frequency planning, high immunity

against interference if a high processing gain is used, and flexible data rate adaptation.

Besides these advantages, DS-SS suffers from several problems in multi-user wireless communications systems with limited available bandwidth [40]:

– *Multiple access interference (MAI)*. As the number of simultaneously active users increases, the performance of the DS-SS system decreases rapidly, since the capacity of a DS-SS system with moderate processing gain (limited spread bandwidth) is limited by MAI.

– *Complexity*. In order to exploit all multi-path diversity it is necessary to apply a matched filter receiver approximated by a rake receiver with a sufficient number of arms. In addition, the receiver has to be matched to the time-variant channel impulse response. Thus, proper channel estimation is necessary. This leads to additional receiver complexity with adaptive receiver filters and a considerable signaling overhead.

– *Single-/multi-tone interference*. In the case of single-tone or multi-tone interference the conventional DS-SS receiver spreads the interference signal over the whole transmission bandwidth B whereas the desired signal part is de-spread. If this interference suppression is not sufficient, additional operations have to be done at the receiver, such as notch filtering in the time domain (based on the least mean square algorithm) or in the frequency domain (based on the fast Fourier transform) to partly decrease the amount of interference [41, 42]. Hence, this extra processing leads to additional receiver complexity.

(2-7) Code Acquisition and Tracking

Before data demodulation and detection can be accomplished in a spread spectrum system, the spreading code must be generated at the receiver (called the local code) and aligned with the received spreading code accounting for delay induced by the channel [36]. The

process of code alignment at the receiver is typically accomplished in two steps: alignment of the local code with the received code to within a fraction of a chip (say 1/10 chip), which is called code acquisition; tracking of the local code with the received code to within a small fraction of a chip (say 1/10 chip or less). There are two main code acquisition techniques: (1) serial search, and (2) matched filter.

For the former, i.e., serial search, an arbitrary starting point is selected in the local code, a trial correlation with the incoming code is performed, the result of this correlation is compared with a threshold, and if the threshold is exceeded, demodulation of the received spread spectrum signal is attempted. If the attempted demodulation fails, or if the threshold was not exceeded by the trial correlation, the local code is delayed a fraction of a chip (typically 1/2 chip), and the process is repeated. This is continued until the tracking of the incoming code by the local code is successful.

For the latter, i.e., matched filter, the magnitude of the output of a filter matched to the spreading code is compared with a threshold. When the threshold is exceeded, it is presumed that this is the delay for which the local and incoming codes are synchronous and the resulting delay is used in the demodulation of the data.

There are advantages and disadvantages to these two techniques. Two main observations are as follows:

- for long codes, serial search is substantially slower than the matched filter method for achieving acquisition.

- the complexity of the construction of the matched filter for matched filter acquisition grows substantially with the length of the spreading code.

Chapter 3: Diversity and RAKE Receiver

(3-1) introduction

One of the most powerful techniques to mitigate the effects of fading is to use diversity-combining of independently fading signal paths. Diversity combining uses the fact that independent signal paths have a low probability of experiencing deep fades simultaneously [39]. Thus, the idea behind diversity is to send the same data over independent fading paths. These independent paths are combined in some way such that the fading of the resultant signal is reduced. When these paths are combined, the fading in one path can be compensated by the received signal from another path. Fig. (3-1) shows how a selected path with the higher signal level from two independent Rayleigh fading paths yields significantly fewer fading periods [43].

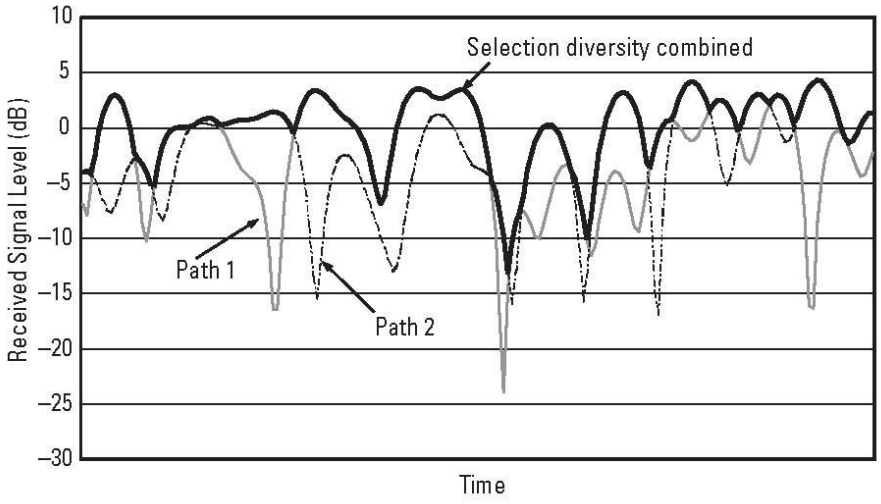

Fig. (3-1) Selection diversity combining of two independent fading patterns.

(3-2) Realization of different diversity schemes

There are many ways of achieving independent fading paths in a wireless system and can be categorized as follow:

- ***Space diversity***: implies creating several independent propagation paths at the expense of involving multiple antennas. Duplicating antennas may be used at the receiving side as well as at the transmitting side. Note that with space diversity, independent fading paths are realized without an increase in transmit signal power or bandwidth. The separation between antennas must be such that the fading amplitudes corresponding to each antenna are approximately independent. That can be achieved by spacing them from each other by a distance of 7-10 wavelength or more [44]. Space diversity can be used at receiver (receive diversity) Fig. (3-2), or used at transmitter (transmit diversity) Fig. (3-3), or can be a combination of both to gain maximal benefits.

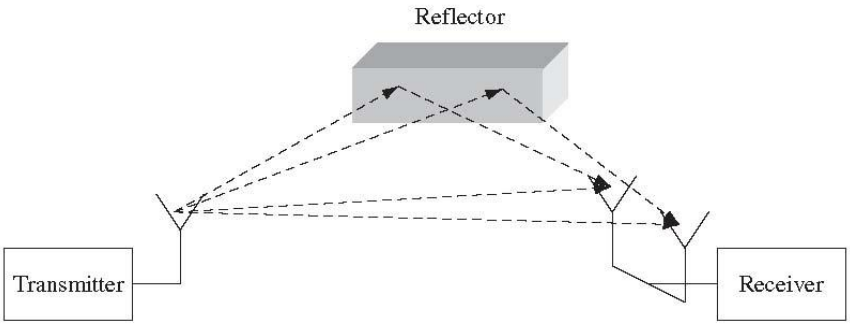

Fig. (3-2) Receive antenna diversity

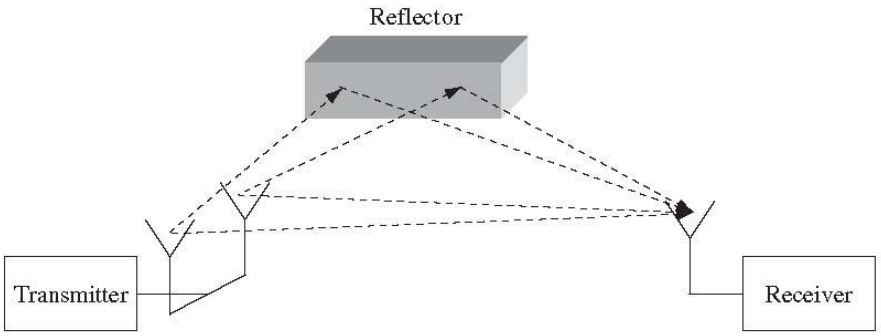

Fig. (3- 3) Transmit antenna diversity

- ***Frequency diversity*:** it is achieved by transmitting the same narrowband signal at different carrier frequencies, where the carriers are separated by the coherence bandwidth of the channel [39]. Spread spectrum techniques are sometimes described as providing frequency diversity since the channel gain varies across the bandwidth of the transmitted signal. However, this is not equivalent to sending the same information signal over independently fading paths.
- ***Time diversity:*** it is achieved by transmitting the same signal at different times, where the time difference is greater than the channel coherence time (the inverse of the channel Doppler spread). Time diversity can also be achieved through coding and interleaving. Clearly time diversity can't be used for stationary applications, since the channel coherence time is infinite and thus fading is highly correlated over time.
- ***Polarization diversity:*** it is achieved by using either two transmit antennas or two receive antennas with different polarization (e.g. vertically and horizontally polarized waves). The two transmitted waves follow the same path however, since the multiple random reflections distribute the power nearly equally relative to both polarizations, the average receive power corresponding to either polarized antenna is approximately the same. There are two disadvantages of polarization diversity. First, you can have at most two

diversity branches, corresponding to the two types of polarization. The second disadvantage is that polarization diversity loses effectively half the power (3 dB) since the transmit or receive power is divided between the two differently polarized antennas, so it has not yet found wide application.

- ***Multipath diversity:*** it is of particular importance to CDMA communication and it is based on the fact that the signals propagating along the different paths reach the receiver with different time delays. In frequency selective channels where the propagation delay spread is larger than the reciprocal of the receiver bandwidth which is the chip period *Tc*, the signals of any two paths with a propagation delay difference of more than *Tc* can be separated and independently detected [45, 46]. These signals also have independent fading patterns.

(3-3) Diversity Combining Methods

A diversity system combines the independent fading paths to obtain a resultant signal that is then passed through a standard demodulator. The combining can be done in several ways which vary in complexity and overall performance.

Most combining techniques are linear: the output of the combiner is just a weighted sum of the different fading paths or branches, as shown in fig. (3-4) for M-branch diversity. Specifically, when all but one of the complex α_is are zero, only one path is passed to the combiner output. When more than one of the α_is is nonzero, the combiner adds together multiple paths, where each path may be weighted by different value. Combining more than one branch signal requires *co-phasing*, where the phase θ_i of the ith branch is removed through the multiplication by $\alpha_i = a_i e^{-j\theta_i}$ for some real-valued a_i. This phase removal requires coherent detection of each branch to determine its phase θ_i. Without co-phasing, the branch signals would not add up coherently in the combiner, so the resulting output could still exhibit significant fading due to constructive and destructive addition of the signals in all the branches.

The multiplication by α_i can be performed either before detection (predetection) or after detection (post-detection) with essentially no difference in performance. Combining is typically performed postdetection, since the branch signal power and/or phase is required to determine the appropriate α_i value. Post-detection combining of multiple branches requires a dedicated receiver for each branch to determine the branch phase, which increases the hardware complexity and power consumption, particular for a large number of branches.

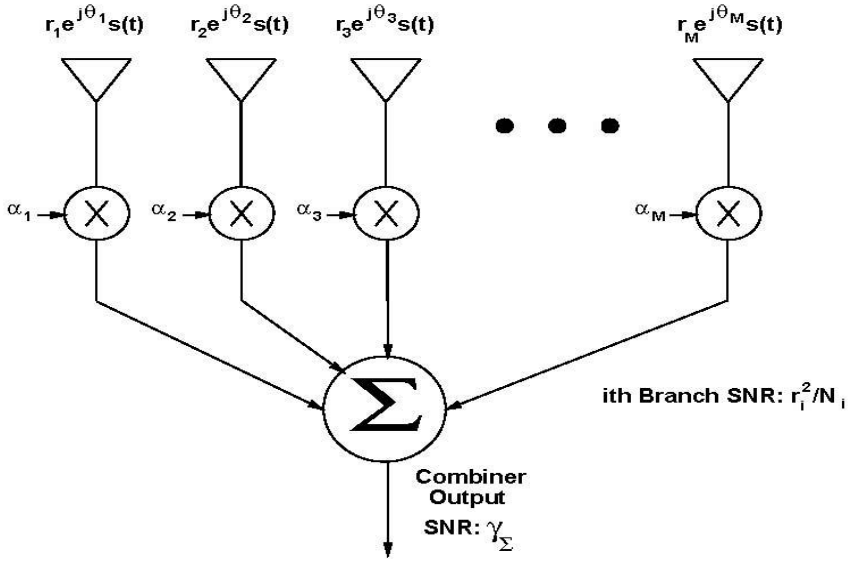

Fig. (3- 4) Linear Combiner

The main purpose of diversity is to combine the independent fading paths so that the effects of fading are mitigated. The signal output from the combiner equals the original transmitted signal *s*(*t*) multiplied by a random complex amplitude term that results from the path combining. This complex amplitude term results in a random SNR γ_Σ at the combiner output, where the distribution of $\boldsymbol{\gamma}_\Sigma$ is a function of the number of diversity paths, the fading distribution on each path, and the combining technique, as shown in more detail below. Since the combiner output is fed into a standard demodulator

for the transmitted signal *s*(*t*), the performance of the diversity system in terms of $\overline{P_s}$ and P_{out} is as defined in [39], i.e.

$$\overline{P_s} = \int_0^{\infty} P_s(\gamma)\, p_{\boldsymbol{\gamma}_\Sigma}(\gamma) d\gamma, \tag{3-1}$$

$$P_{out} = p\left(\gamma_\Sigma \leq \gamma_{\mathbf{0}}\right) = \int_0^{\gamma_{\mathbf{0}}} p_{\boldsymbol{\gamma}_\Sigma}(\gamma) d\gamma, \tag{3-2}$$

For some target SNR value $\gamma_{\mathbf{0}}$, where P_s is the symbol error probability, $\overline{P_s}$ the averaged probability of error, P_{out} is the outage probability, $P_s\left(\gamma_\Sigma\right)$ is the probability of symbol error for demodulation of *s*(*t*) in AWGN with SNR γ_Σ **,** and $p_{\boldsymbol{\gamma}_\Sigma}(\gamma)$ is the probability distribution of random variable $\boldsymbol{\gamma}_\Sigma$.

Next we describe different combining techniques and their performance

(3-3-1) Selection Combining

In selection combining (SC), the combiner outputs the signal on the branch with the highest SNR r_i^2/N_i . This is equivalent to choosing the branch with the highest $r_i^2 + N_i$ if the noise $N_i = N$ is the same on all branches. Since only one branch is used at a time, SC often requires just one receiver that is switched into the active antenna branch. However, a dedicated receiver on each antenna branch may be needed for systems that transmit continuously in order to simultaneously and continuously monitor SNR on each branch. With SC the path output from the combiner has an SNR equal to the maximum SNR of all the branches. Moreover, since only one branch output is used, co-phasing of multiple branches is not required, so this technique can be used with either coherent or differential modulation. From [39] For *M* branch diversity, we see that the outage probability of the selection-combiner for a target γ_0 is

$$P_{out}(\gamma_0) = \prod_{i=1}^{M}\left[1 - e^{-\gamma_0/\overline{\gamma}_i}\right] \tag{3-3}$$

If the average SNR for all of the branches are the same ($\overline{\gamma_i}= \overline{\gamma}$ for all *i*), then this reduces to

$$P_{out}(\gamma_0) = \left[1 - e^{-\gamma_0/\overline{\gamma}}\right]^M \tag{3-4}$$

And the average SNR of the combiner output in independent and identically distributed (i.i.d.) Rayleigh fading is

$$\bar{\gamma}_{\sum} = \bar{\gamma} \sum_{i=1}^{M} \frac{1}{i} \tag{3-5}$$

Where $\bar{\gamma}$ the average SNR on the ith branch. Thus, the average SNR gain increases with M, but not linearly. The biggest gain is obtained by going from no diversity to two-branch diversity. This is shown in Fig. (3-5), which shows P_{out} versus $\bar{\gamma}/\,\boldsymbol{\gamma_0}$ for different *M* in i.i.d. Rayleigh fading.

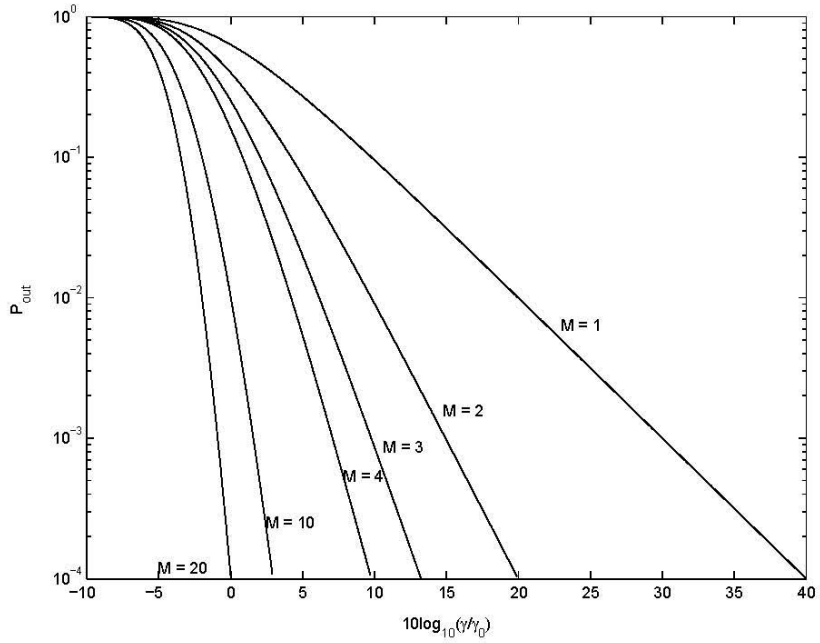

Fig. (3- 5) outage probability of selection combining in Rayleigh fading

(3-3-2) Threshold Combining

SC for systems that transmit continuously may require a dedicated receiver on each branch to continuously monitor branch SNR. A simpler type of combining, called threshold combining, avoids the need for a dedicated receiver on each branch by scanning each of the branches in sequential order and outputting the first signal with SNR above a given threshold γ_T . As in SC, since only one branch output is used at a time, co-phasing is not required. Thus, this technique can be used with either coherent or differential modulation.

Once a branch is chosen, as long as the SNR on that branch remains above the desired threshold, the combiner outputs that signal. If the SNR on the selected branch falls below the threshold, the combiner switches to another branch. There are several criteria the combiner can use to decide which branch to switch to [47]. The simplest criterion is to switch randomly to another branch. With only two-branch diversity this is equivalent to switching to the other branch when the SNR on the active branch falls below γ_T. This method is called **switch and stay combining** (SSC). The switching process and SNR associated with SSC is illustrated in Figure 4.6. Since the SSC does not select the branch with the highest SNR, its performance is between that of no diversity and ideal SC.

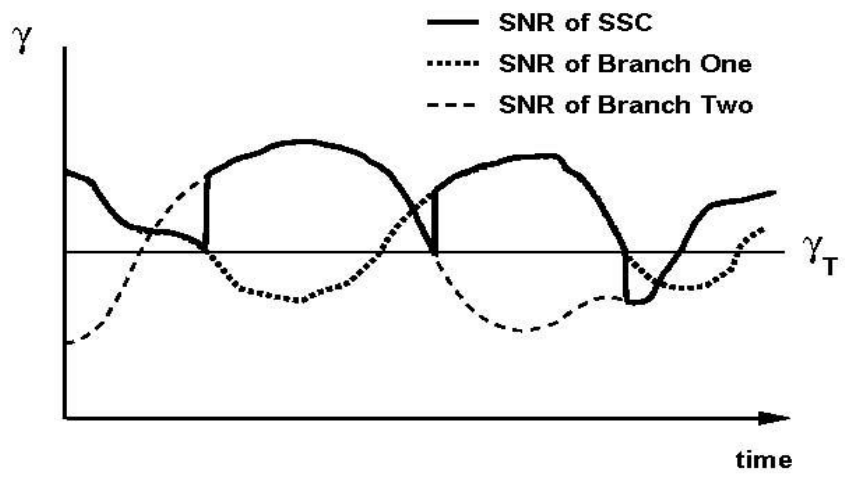

Fig. (3- 6) SNR of SSC Technique.

The outage probability P_{out} associated with a given γ_0 is given by

$$P_{out}(\gamma_0) = \begin{cases} 1 - e^{-\frac{\gamma_T}{\bar{\gamma}}} - e^{-\frac{\gamma_0}{\bar{\gamma}}} + e^{-\frac{(\gamma_T+\gamma_0)}{\bar{\gamma}}} & \gamma < \gamma_T \\ 1 - 2e^{-\frac{\gamma_0}{\bar{\gamma}}} + e^{-\frac{(\gamma_T+\gamma_0)}{\bar{\gamma}}} & \gamma \geq \gamma_T \end{cases}$$

(3-6)

The performance of SSC under other types of fading, as well as the effects of fading correlation, is studied in [48] and it is shown that for any fading distribution, SSC with an optimized threshold has the same outage probability as SC.

(3-3-3) Maximal Ratio Combining

In SC and SSC, the output of the combiner equals the signal on one of the branches. In maximal ratio combining (MRC) the output is a weighted sum of all branches, so the α_is in Fig. (3-4) are all nonzero. Since the signals are cophased, $\alpha_i = a_i e^{-j\theta_i}$, where θ_i is the phase of the incoming signal on the ith branch. Thus, the envelope of the combiner output will be $r = \sum_{i=1}^{M} a_i r_i$. Assuming the same noise power N in each branch yields a total noise power N_{tot} at the

combiner output of $N_{tot} = \sum_{i=1}^{M} a_i^2 N$. Thus, the output SNR of the combiner is

$$\gamma_{\sum} = \frac{r^2}{N_{tot}} = \frac{1}{N} \frac{\left(\sum_{i=1}^{M} a_i r_i\right)^2}{\sum_{i=1}^{M} a_i^2}. \quad (3\text{-}7)$$

α_is is chosen to maximize $\gamma_{\sum}$ [10] which will be

$$\gamma_{\sum} = \sum_{i=1}^{M} \frac{r_i^2}{N} = \sum_{i=1}^{M} \gamma_i \quad (3\text{-}8)$$

Thus, the SNR of the combiner output is the sum of SNRs on each branch. The average combiner SNR increases linearly with the number of diversity branches *M*, in contrast to the diminishing returns associated with the average combiner SNR in SC.

Assuming i.i.d. Rayleigh fading on each branch with equal average branch SNR $\bar{\gamma}$, the distribution of $\gamma_{\sum}$ is given by

$$p_{\gamma_{\sum}}(\gamma) = \frac{\gamma^{M-1} e^{-\gamma/\bar{\gamma}}}{\bar{\gamma}^M (M-1)!}, \quad \gamma \geq 0. \quad (3\text{-}9)$$

The corresponding outage probability for a given threshold γ_0 is given by

$$P_{out} = p(\gamma_{\sum} < \gamma_0) = \int_0^{\gamma_0} p_{\gamma_{\sum}}(\gamma) d\gamma = 1 - e^{-\gamma_0/\bar{\gamma}} \sum_{k=1}^{M} \frac{(\gamma_0/\bar{\gamma})^{k-1}}{(k-1)!}.$$

(3-10)Fig. (3-7) plots *Pout* for maximal ratio combining indexed by the number of diversity branches. Comparing the outage probability for MRC with that of SC in indicates that MRC has significantly better performance than SC.

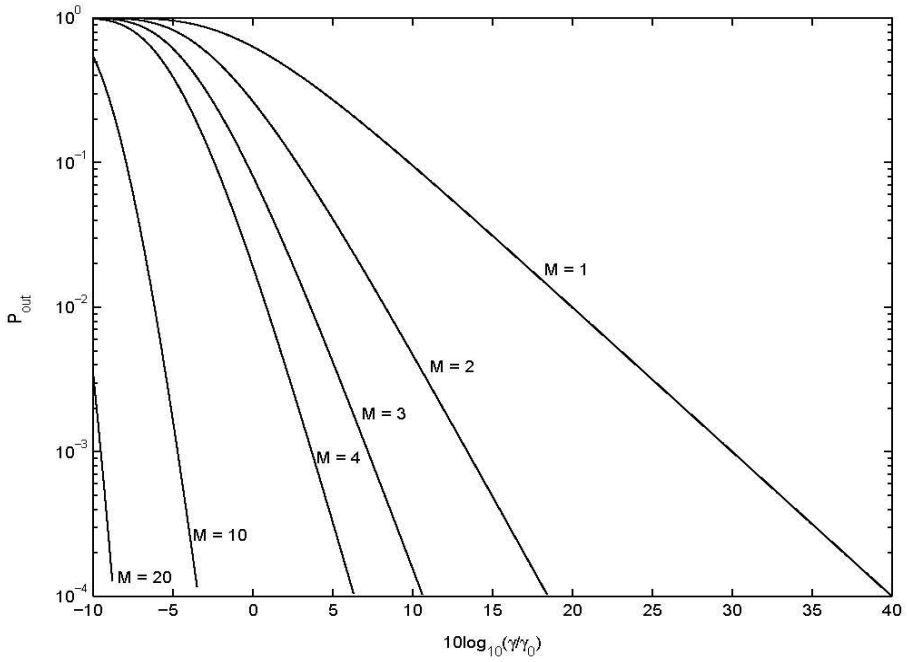

Fig. (3- *7) Pout* for MRC with i.i.d. Rayleigh fading.

(3-3-4) Equal-Gain Combining

MRC requires knowledge of the time-varying SNR on each branch, which can be very difficult to measure. A simpler technique is equal-gain combining (EGC), which co-phases the signals on each branch and then combines them with equal weighting, $\alpha_i = e^{-\theta_i}$. The SNR of the combiner output, assuming equal noise power N in each branch, is then given by

$$\gamma_{\Sigma} = \frac{1}{NM} \left(\sum_{i=1}^{M} r_i\right)^2. \tag{3-11}$$

For i.i.d. Rayleigh fading and two-branch diversity and average branch SNR $\bar{\gamma}$, an expression for the CDF (cumulative distribution function) in terms of the *Q* function can be derived as [49][50]

$$P_{\gamma_{\Sigma}}(\gamma) = 1 - e^{-2\gamma/\bar{\gamma}} \sqrt{\frac{\pi\gamma}{\bar{\gamma}}}\, e^{-\gamma/\bar{\gamma}} \left(1 - 2Q\left(\sqrt{2\gamma/\bar{\gamma}}\right)\right) \tag{3-12}$$

Then the resulting outage probability is given by

$$P_{out}(\gamma_0) = 1 - e^{-2\gamma_R} - \sqrt{\pi\gamma_R}e^{-\gamma_R}\left(1 - 2Q\left(\sqrt{2\gamma_R}\right)\right) \quad (3\text{-}13)$$

Where $\gamma_R = \gamma_0/\bar{\gamma}$. It is shown in [49] that performance of EGC is quite close to that of MRC, typically exhibiting less than 1 dB of power penalty. This is the price paid for the reduced complexity of using equal gains.

(3-4) Diversity and Spread Spectrum

Some form of diversity is crucial in compensating for the effects of fading. Spread-spectrum systems exploit the different types of diversity that are available. A direct-sequence receiver exploits time diversity through the small number of branches or demodulators in its RAKE receiver [51]. These demodulators must be synchronized to the path delays of the multipath components. The effectiveness of the rake receiver depends on the concentration of strong diffuse and specular components in the vicinity of resolvable path delays, which becomes more likely as the chip rate increases.

(3-5) RAKE Receiver

A rake receiver is a radio receiver designed to counter the effects of multi path fading [52]. It does this by using several "sub-receivers" each delayed slightly in order to tune in to the individual multi path components. Each component is decoded independently, but at a later stage combined in order to make the most use of the different transmission characteristics of each transmission path. This achieves a significant improvement in the SNR of the output signal. The RAKE receiver however, works only on the basis that these multipath components are practically uncorrelated from one another when their relative propagation delays exceed a chip period [53]. Rake receivers are common in a wide variety of radio devices, including mobile phones and wireless LAN (local area network) equipment.

Fig (3-8) shows the model of a RAKE receiver with three correlators. This RAKE receiver design is used in the IS-95 system, where each of the three strongest time-shifted multipath signals is demodulated and weighted independently. The number of available RAKE fingers depends on the channel profile and the chip rate. The higher the chip rate, the more resolvable paths there are, but higher chip rate will cause wider bandwidth. To catch all the energy from the channel more RAKE fingers are needed. A very large number of fingers lead to combining losses and practical implementation problems. Note that in a RAKE receiver, if the outputs from one correlator are corrupted by fading, the corrupted signal may be discounted through the weighting process. Decisions based on the combination of the three separate correlator outputs are able to provide a form of diversity, which can overcome fading and thereby improve the CDMA reception [53].

Each correlator of the RAKE receiver is represented by three coefficients: (1) Time delay; (2) Phase shift; (3) Amplitude gain/attenuation, as shown in figure 3.8. The spreading code in the despreading process needs to be synchronized to the delay spread of the multipath signal, so that the outputs of each correlator can be summed to produce a stronger and more accurate signal. Impulse response measurements of the multi path channel profile are executed through a matched filter to make a successful de-spreading. It reveals multi path channel peaks and gives timing and RAKE finger allocations to different receiver blocks and tracking and monitoring these peaks later. The code generator of each finger is adjusted to generate a code sequence with a specific offset, which corresponds to the detected multipath. The generated code sequence is supplied to the correlator, which despreads the corresponding multipath. The correlation is obtained by multiplying the received sequence chips with corresponding chips of the spreading sequence and summing them up. By means of channel estimation the gain and phase needed for combining are determined. Finally the bit decision is made using the combined output.

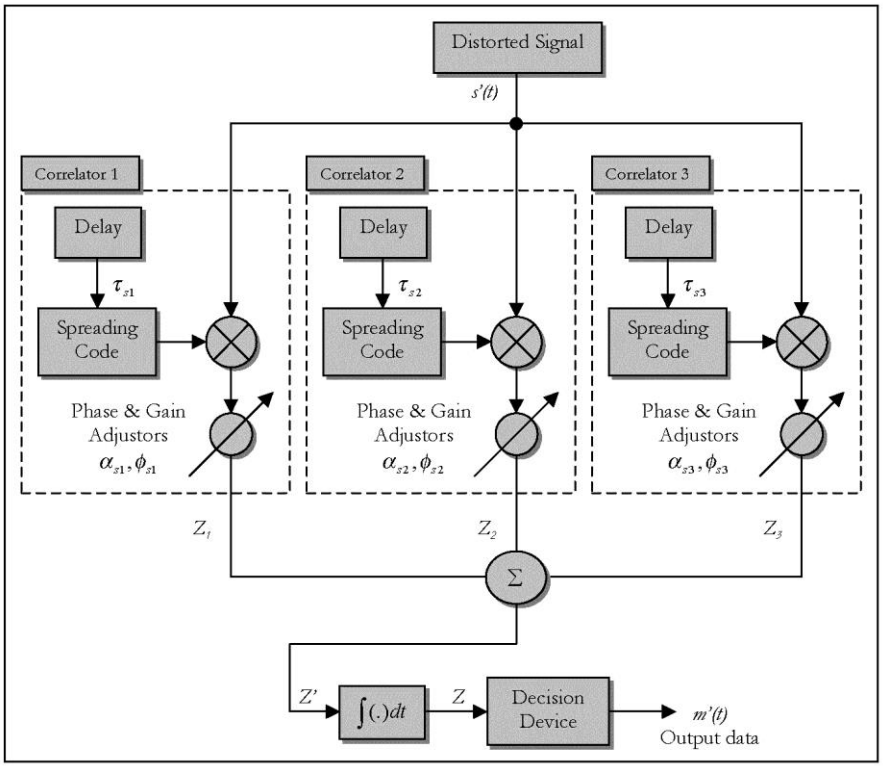

Fig. (3- 8)An implementation of a RAKE receiver with 3 correlators

We can summarize the functions contained in RAKE receiver as follow:

1. Channel delay estimation for multipath components.

2. RAKE receiver finger allocation based on the channel delay estimation.

3. RAKE receiver fingers to perform the despreading operation.

4. Adaptive channel estimation.

5. Combining (MRC technique is the most used).

There are three main types of rake receiver [54]:

The All rake (A-rake), the Selective rake (S-rake), and the Partial rake (P-rake).

The All Rake: The A-rake receiver captures and combines all the multipath components of the channel by having a number of rake fingers equal to their number. This structure is only theoretical for most systems, since the number of multipath components is too large to implement this type of rake receiver. Nevertheless, it can be used for simulation purposes to determine the optimal achievable performance of any system.

The Selective Rake: The S-rake receiver is a more practical and implementable structure. Its fingers capture and combine only the strongest multipath components. It requires a-posteriori channel estimation to do so. This kind of rake maximizes the SNR.

The Partial Rake: The P-rake receiver is a simplified version of the S-rake. Its fingers capture and combine only the first multipath components. The dichotomy is that it does not require channel information, but, the multipath components combined are not always the strongest ones and therefore performance compared to the S-rake structure is reduced.

(3-6) Fading channel estimation

The estimation of channel taps plays a key role in the performance of the RAKE receiver as discussed by [55, 58, 59, and 60]. Alouini et. al. [60] have shown that imperfect or inaccurate channel estimation leads to a serious degradation in the performance of MRC based RAKE receivers and in that case equal gain combining can perform better.

Fading channels are characterized as random time-varying systems. Thus the estimation of the fading channel impulse response belongs to a more general class of time-varying system identification problem [60, chapter 16]. Beside the rich literature of system identification, a

large number of researchers have attempted the problem of fading channel estimation separately [61, 62, 63 and 64]. Among other techniques, adaptive filtering is the most common technique that is widely used for fading channel estimation [65].

The techniques that do not attempt to model the fading channels explicitly reduce the error risk and complexity of the algorithm. These techniques generally use LMS or RLS algorithm to adapt the filter taps. The advantage of LMS algorithm over RLS is its simplicity of implementation and suitability for this problem. In general, the LMS algorithm exhibits more robust tracking behavior than the standard RLS algorithm [66, 67]. Because of these features LMS algorithm is selected for the estimation of multipath channel in this thesis. A sequence of reference data is usually needed to train the adaptive filter. In CDMA systems, a known pilot symbol sequence can be used for this purpose.

(3-6-1) Overview of the LMS Adaptive Filter

The LMS algorithm was first proposed by Widrow and Hoff at the Stanford University in 1960 [68]. Until now, the algorithm is still widely used due to its simplicity and cheap implementation [60]. The LMS algorithm is seen as having low computational complexity, good stability properties, relatively good robustness against implementation errors and simplicity of its behavior.

The system considered is shown in fig. (3-9). This system describes the estimation of an unknown channel through the implementation of the LMS adaptive filtering via parallel configuration [69]. Both the unknown channel and the adaptive FIR filter model are excited by a training sequence, *u(k).* The adaptive FIR filter output, *yy(k)* is compared with the unknown channel output, *y(k)* to produce the error signal, *e(k).* This error represents the difference between the unknown channel and the model output, which is also equivalent to the noise, *nn(k)* added into the system. The error signal is then inputted to the LMS adaptive algorithm, which corrects the individual tap weights of the filter. This process is repeated through this

implementation, the noise in the channel is effectively cancelled and the resultant FIR filter response now closely represents that of the previously unknown channel. several iterations until the error signal becomes sufficiently small.

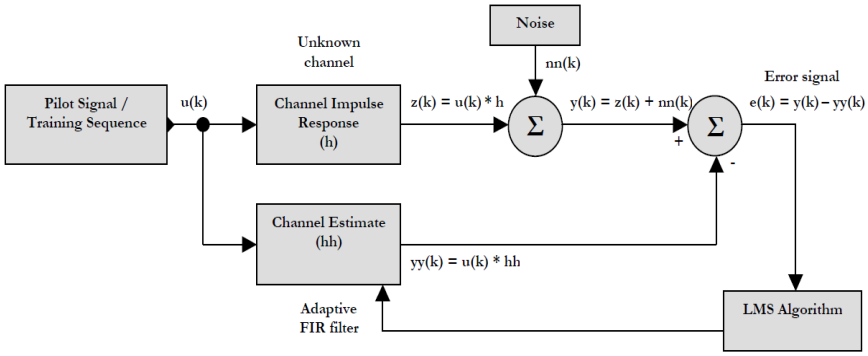

Fig. (3- 9) LMS adaptive FIR filter in parallel with the time invariant unknown channel

(3-6-2) Derivation of the Standard LMS Algorithm [69], [70], [71], [72]

From fig. (3-9), the unknown channel is modelled by a FIR filter, $h(z^{-1})$ and is given by:

$$h(z^{-1}) = h_0 + h_1 z^{-1} + \cdots + h_{n-1} z^{-n+1} \quad (3\text{-}14)$$

Where z^{-1} is the unit delay operator and n is the tap length. The LMS adaptive FIR filter, *hh* has a tap delay line structure given by:

$$hh(z^{-1}) = hh_0 + hh_1 z^{-1} + \cdots + hh_{m-1} z^{-m+1} \quad (3\text{-}15)$$

Where *m* is the tap length for the adaptive filter. All tap coefficients of *hh(k)* are initially set to zero. The training sequence, *u(k)* and noise, *nn(k)* is assumed to be a zero mean wide sense stationary process and that these two signals are uncorrelated with each other. The observed output from the unknown channel is given by:

$$z(k) = u(k) \otimes h \tag{3-16a}$$

or

$$z(k) = U(k)^T . h \tag{3-16b}$$

Where $\otimes$ means the convolution function and

$$U(k) = [u(k) \quad u(k-1) \ldots \ldots u(k-n+1)]^T \tag{3-17}$$

The channel output obtained from equation (3-16b) is additive to the noise, *nn(k)* and the output signal *y(k)* is given by:

$$y(k) = U(k)^T .\ h + nn(k) \tag{3-18}$$

The output from the adaptive filter is given by:

$$yy(k) = U(k)^T .\ hh \tag{3-19}$$

Where

$$hh = [hh_0 \quad hh_1 \quad \ldots \quad hh_{n-1}]^T \tag{3-20}$$

The output of the adaptive filter is subtracted from the output of the unknown channel to obtain the error signal, *e(k)*:

$$e(k) = y(k) - yy(k) = U(k)^T .\ (h - hh) + nn(k) \tag{3-21}$$

The error signal, *e(k)* obtained in equation (3-21) shall ideally be equal to the noise, *nn(k)*. This will mean that the LMS algorithm has successfully estimated the unknown channel, *h*. The LMS algorithm updates as the tap coefficients by weighting them using the equation:

$$hh(k+1) = hh^*(k) + \mu .\ e^*(k) .U(k) \tag{3-22}$$

where * is the complex conjugate, *U(k)* is the training sequence vector obtain from equation (3-17) and μ is known as the adaptation parameter or the step size factor. The step size, μ is a major parameter in the LMS algorithm derived in equation (3-22). This parameter is considered important as it influences the convergence and stability rate of the LMS adaptive filter [60]. A smaller μ results in a slower convergence rate but have a more accurate and stable

result, while a larger μ have a faster convergence rate but leads to an unstable system. The selection of the step size, μ is therefore crucial for its performance to provide a good convergence rate and stability in the system. The LMS algorithm will converge and remain stable as long as the step size fulfills the range given by:

$$0 < \mu < \frac{2}{\sum_{i=k-n+1}^{k} u^2(i)} \tag{3-23}$$

Where *k* is the current time interval and *n* is the tap length

Chapter 4: MATLAB Models and Simulation Results

(4-1) Introduction

Some time ago, the Defense Department adopted a procurement policy "fly before you buy". In the modern world of telecommunications the equivalent concept might be termed "simulate before you build". The economics associated with the link performance are quite severe. Even a small degradation will affect the system data rate or coverage, both of which are related to capital and operating expenses. It is crucial to have all of the system design parameters optimized before a heavy commitment to implementation [73]. Furthermore, when things go wrong in the actual article during construction or initial operation, a simulation model can be used to track down the offending element. The simulation will also be useful for pre-testing any corrective action before attempting it in real.

In this thesis, we use MATLAB-SIMULINK toolboxes to simulate a complete system of a DSSS system in a time varying channel using Rake receiver, evaluate its performance, and show the improvement that Rake receiver makes in its performance. The MATLAB models are presented in this chapter and the results are shown and analyzed part by part starting from the modeling of a simple DSSS system in an AWGN channel until the development of the whole system.

We can summarize the simulation phases as follow:

1. Building a DSSS model with BPSK modulation via AWGN channel.
2. Adding multipath to the channel with defined delays and testing different number of rake fingers.
3. Testing different combinations of multipath delays to show the effect of the change in delay spread.
4. Providing channel estimation for a stationary channel and testing different pilot signals with different lengths.
5. Using time varying channel with different variation rates.

(4-2) Phase 1: A DSSS system with BPSK modulation

The first step in our work was building a DSSS system with BPSK modulation. We first used a passband BPSK and tracked the signal at each block end and got some waveforms to see how close is our model behavior to the theoretical one (review sec (2-)) and to get more understanding for the system flow.

(4-2-1) Matlab model

Fig (4-1) illustrates the constructed simulink model with all details and no subsystems.

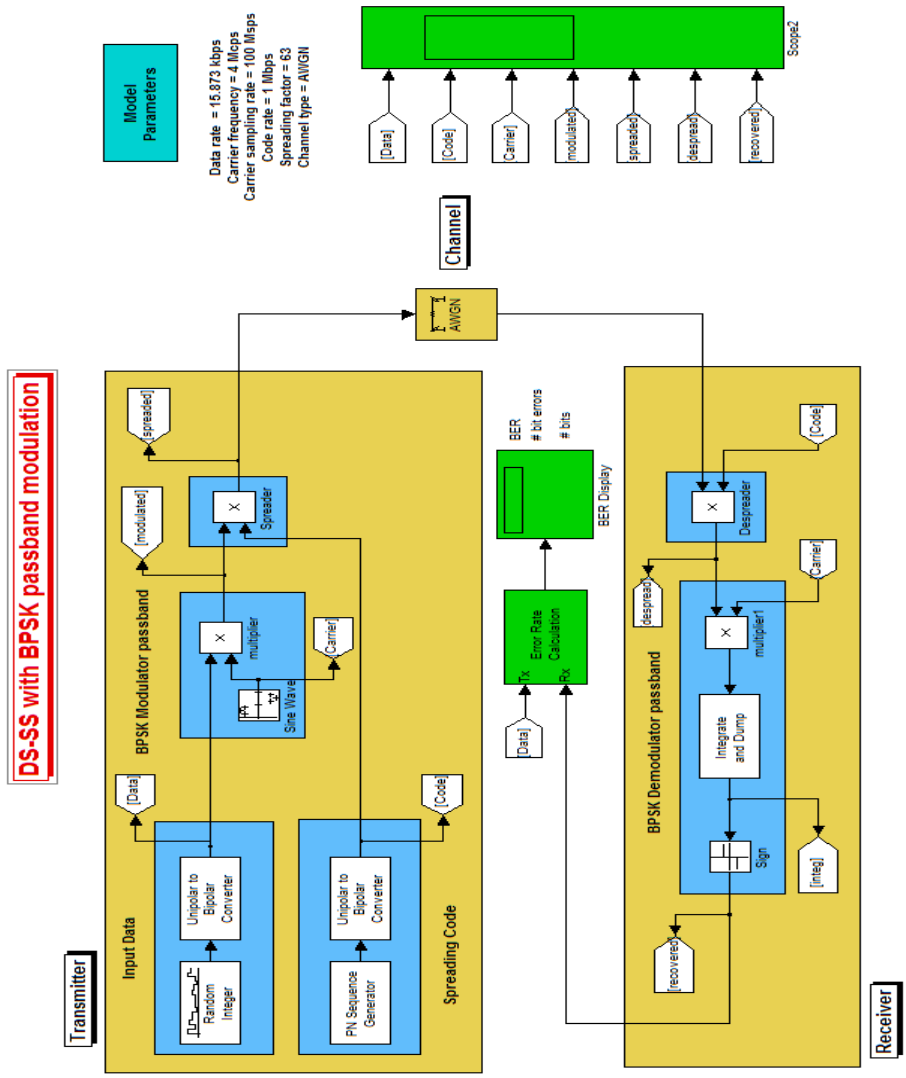

Fig. (4- 1) Matlab model for DSSS system with BPSK passband modulation

(4-2-2) Exploring the model

Now, we will explore our model by stating the functions implemented and the used blocks and their corresponding settings. They can be listed as follows:

i. ***Generating binary data stream****:* By using *Random integer generator* block in the communication tool box, we generated binary data stream of 15.837Kbps data rate followed by a *unipolar to bipolar* block to convert it to NRZ format.

ii. ***Generating spreading code****:* by using *PN sequence generator* block we got a 63-bit sequence of 1Mcps chip rate followed by *a unipolar to bipolar* block.

iii. ***Generating the carrier****:* by using *sine wave* block we had a sinusoidal wave of a frequency 4Mcycle/sec and sampling rate 100Msample/sec.

iv. ***BPSK modulation****:* we used the *product* block which outputs the result of multiplying two inputs.

v. ***Spreading****:* multiplication is also accomplished using *product* block.

vi. ***Adding noise****:* by using *AWGN channel* block. It adds white Gaussian noise to the transmitted signal. We used E_b/N_o range from 0dB to 12 dB.

vii. ***Despreading****:* as for spreading, we used a *product* block and we used the same spreading code for despreading to ensure perfect synchronization.

viii. ***BPSK demodulation****:* we used *product* block for multiplication using the same carrier signal for the sake of synchronization, followed by an *integrate and dump* block

which Integrates over the number of samples in the integration period and reset at the end of the integration, then we used a *signum* block as the final decision device.

ix. ***Bit error rate calculation****:* by using *error rate calculation* block which computes the error rate of the received data by comparing it to a delayed version of the transmitted data. The block output is a three-element vector consisting of the error rate, followed by the number of errors detected and the total number of symbols compared.

x. ***Results and displays****:* we can use a *display* block for visualizing the BER outputs, and a *scope* block for different signals waveforms.

(4-2-3) simulation results

The simulation results at each step are shown below. The results are displayed in the form of snapshots of scope signals.

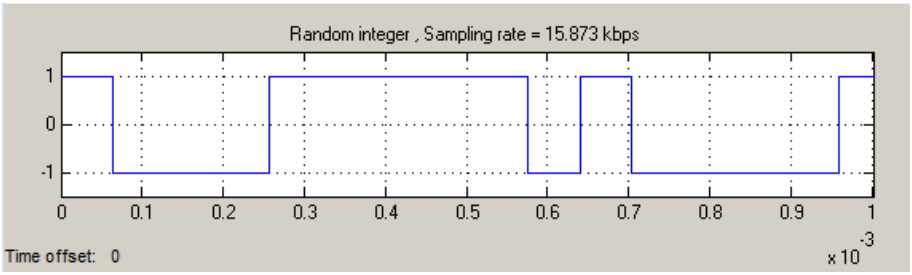

Fig. (4- 2) Input bit stream in bipolar form

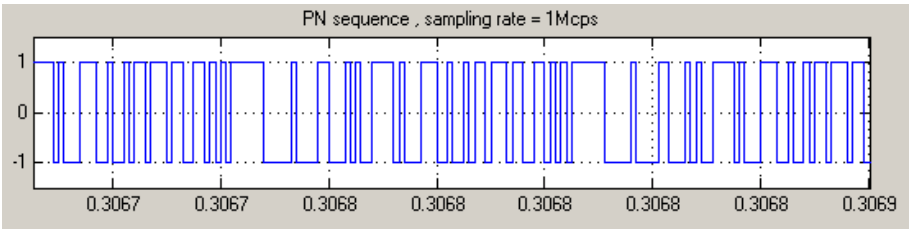

Fig. (4- 3) PN code in bipolar form

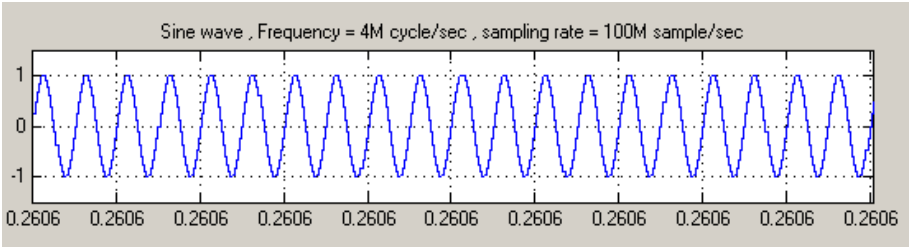

Fig. (4- 4) Carrier signal

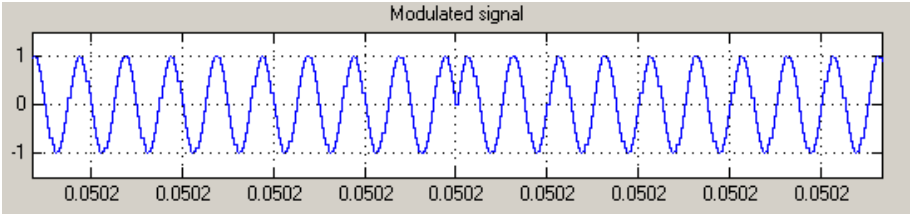

Fig. (4- 5) Modulated signal

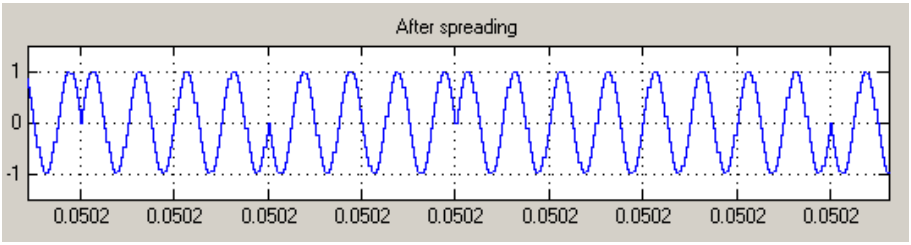

Fig. (4- 6) Spreaded signal

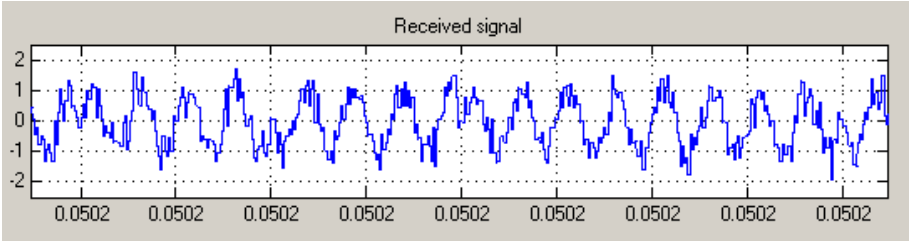

Fig. (4- 7) Received signal at 3dB Eb/No

Fig. (4- 8) Signal after despreading

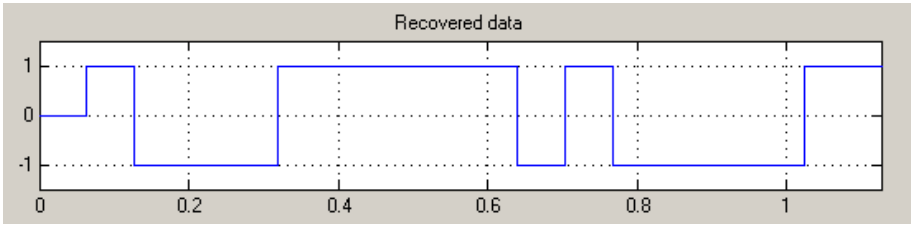

Fig. (4- 9) Recovered data

(4-2-4) problems and tuning

After examining the model and investigating the simulation results we found The model working fine and the waveforms look as expected, but there was a problem that BER was always equal zero which doesn't match the theoritical BER shown in figure below.

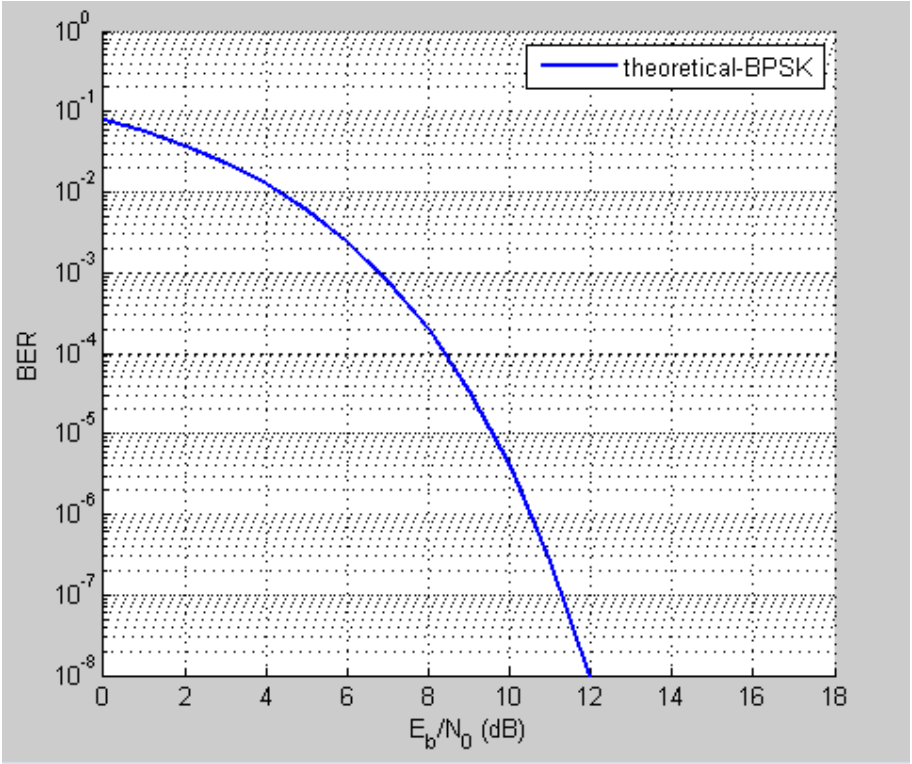

Fig. (4- 10) Theoritical BER for BPSK modulation

The problem was solved by adding a *normalizing gain* equals by $1/\sqrt{SF}$ before signal transmission. The modified model is shown below. We replaced tha BPSK passband modultion with baseband modulation for simplicity.

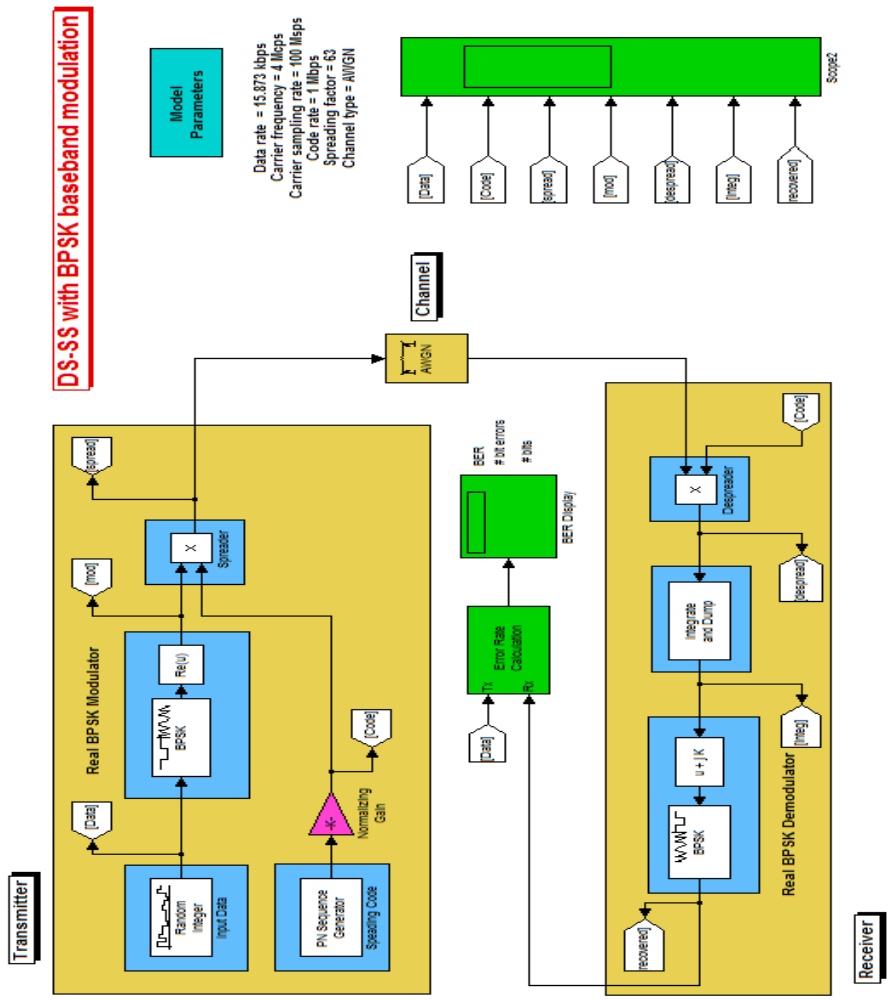

Fig. (4- 11) Modified matlab model for DSSS system with BPSK baseband modulation

(4-2-5) BER performance

To investigate the modified model performance, we compared its BER to the theoritical one. This is done using *bertool*. BERTool is a bit error rate analysis application for analyzing communication systems' bit error rate (BER) performance. Using BERTool we can:

- generate BER data for a communication system using:
    - Closed-form expressions for theoretical BER performance of selected types of communication systems. This is usually used as a reference in ber comparison.
    - The semianalytic technique.
    - Simulations contained in MATLAB simulation functions or Simulink models. After we create a function or model that simulates the system, BERTool iterates over our choice of Eb/No values and collects the results.
- Plot one or more BER data sets on a single set of axes.
- Fit a curve to a set of simulation data.
- Send BER data to the MATLAB workspace or to a file for any further processing we might want to perform.

In our model we used an Eb/No range from 0dB~12dB and the results are shown in the figure below. It is now clear from the BER mapping that our model is perfectly tracking the theoritical BER.

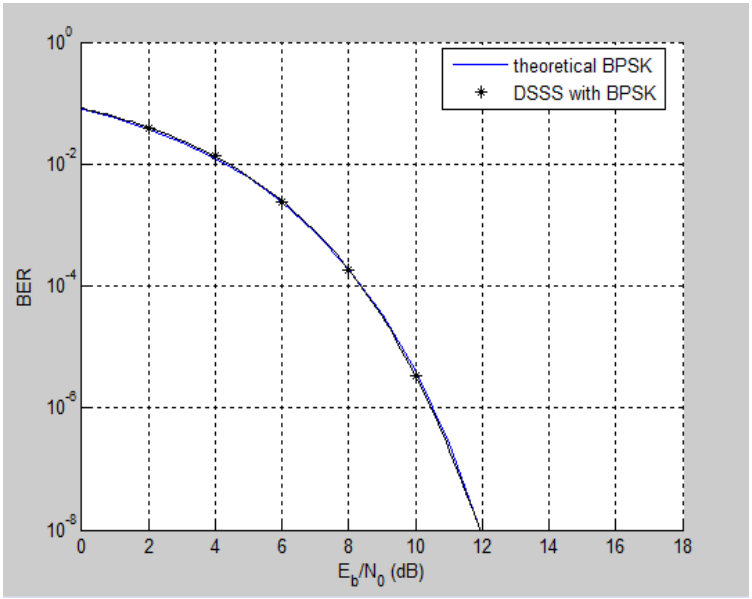

Fig. (4- 12) BER comparison between DSSS system and theoritical

(4-3) Phase 2: Adding multipath channel and RAKE receiver

We have now a working DSSS model with a good performance. The next step is to add the multipath effect to the channel and introduce the rake receiver sarting with one rake finger till we reach the number of all paths. We shall see the improvement in BER when increasing number of rake fingers. We assume prior knowledge of the number of multipath and the delays encountered by them. A simple model showing the multipath channel and rake receiver is shown below. We assume equal gains and no phase distortion.

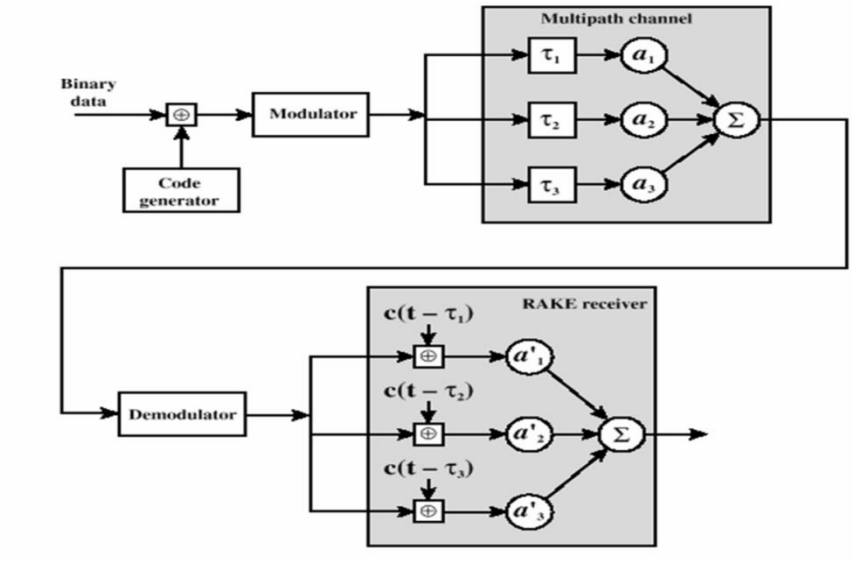

Fig. (4- 13) Principle of RAKE receiver

(4-3-1) Matlab model

We started from the point we had reached. Two modifications were performed to the model:

- Adding multipath to the channel.
- Adding rake combiner to the receiver.

This is shown in the figure below.

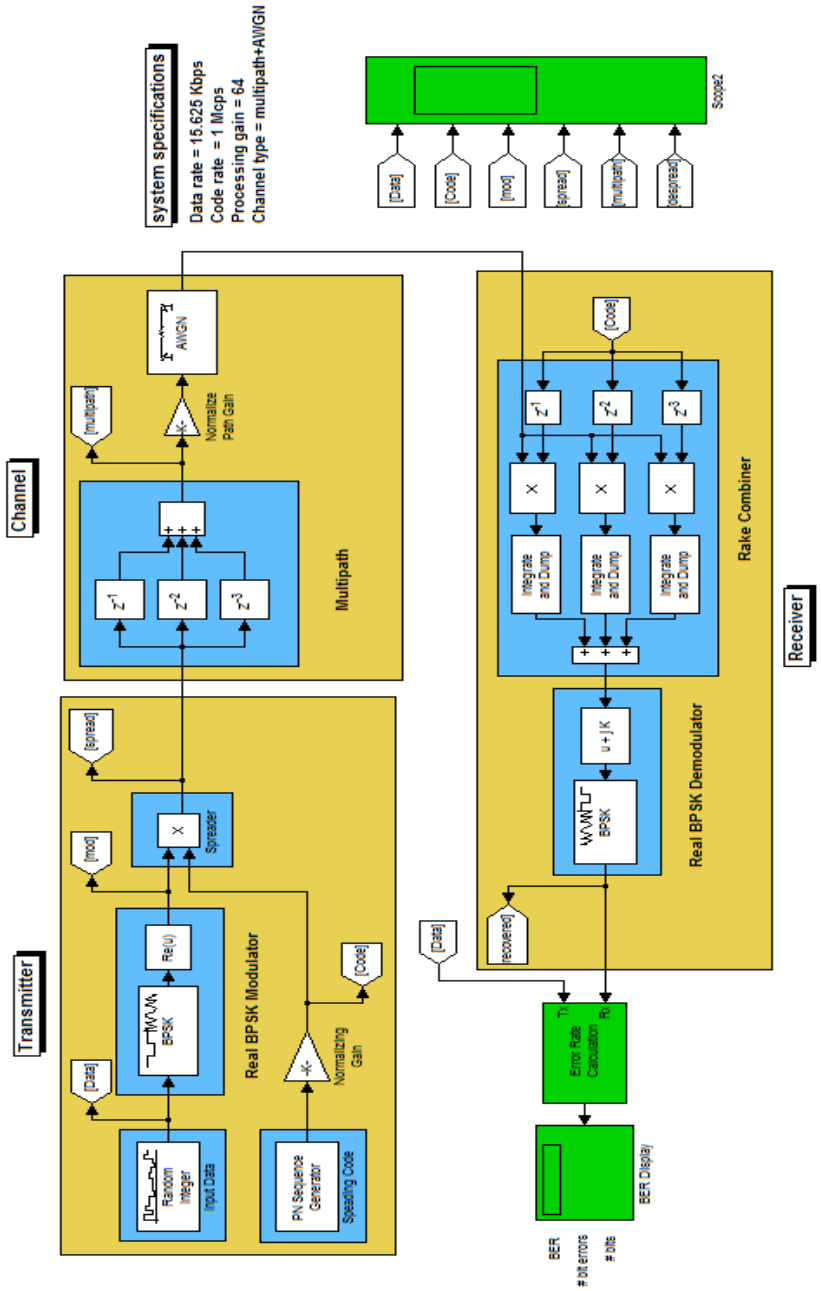

Fig. (4- 14) Matlab model for DSSS system in a multipath channel using Rake receiver

(4-3-2) exploring the model

i. ***Generating binary data stream****:* By using *Random integer generator* block, we generated binary data stream of 15.625Kbps data rate.

ii. ***Generating spreading code****:* by using *PN sequence generator* block we got a 64-bit sequence of 1Mcps chip rate.

iii. ***BPSK modulation****:* we used *BPSK modulator baseband* block which modulates the input signal using the binary phase shift keying method, followed by a *complex to Real-Imag* block to have a real state output.

iv. ***Spreading****:* multiplication is accomplished using *product* block.

v. ***Adding multipath****:* to add the multipath fading effect to the channel, we constructed 3 paths to the transmitted signal each delayed by a certain value using a *delay* block which Delays input by a fixed or variable number of samples. These blocks are set to 1, 2, 3 chips. The 3 paths are then added together using *sum* block and multiplied by 1/3 by a *gain* block to normalize path gain. We finally added noise by *AWGN* block.

vi. ***Rake combiner****:* For the 3 multipath channel, we need a 3 fingers rake receiver, so the received signal passes through 3 correlators each consists of a despreader and an integrator. The despreading code must be delayed by the defined values of multipath delays. Then the 3 fingers are equally gain combined by a *sum* block.

vii. ***BPSK demodulation****:* we first put a *Real-Imag to complex* block to transform the combined signal into complex, then we used a *BPSK demodulator baseband* block. By using a real BPSK modulator, we didn't need a decision device.

viii. Bit error rate calculation: same as previous model.

ix. **Results and displays**: same as previous model
.

(4-3-3) BER performance

Simulations are carried out to evaluate the BER performance of the constructed model. Four simulations are performed to compare between 4 cases:

1. Presence of multipath fading without using Rake.
2. Using one finger Rake.
3. Using two fingers Rake.
4. Using three fingers Rake.

We should see an improvement in BER with increasing the number of Rake fingers. This is illustrated in the following BER comparison. We repeated the same procedures using Hadamard code instead of PN code.

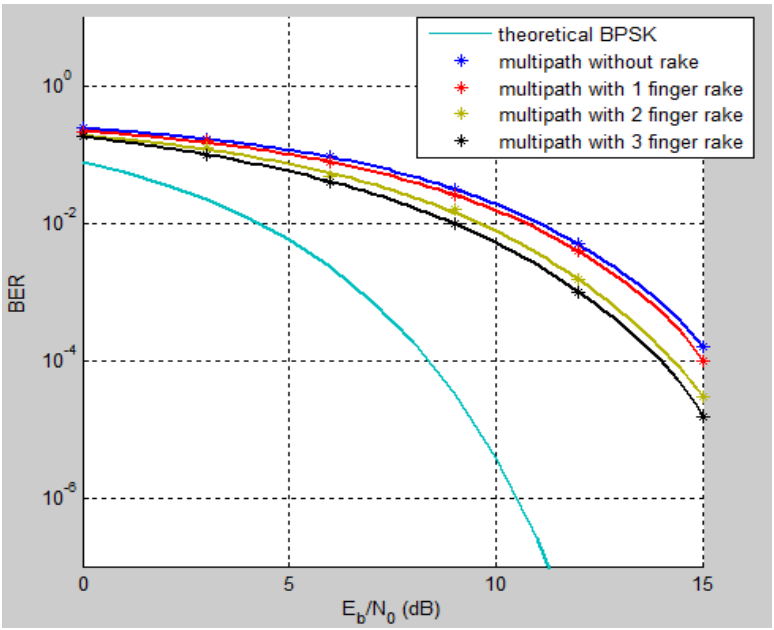

Fig. (4- 15) BER comparison between theoritical BPSK and simulation results of model (4-14) with/without Rake

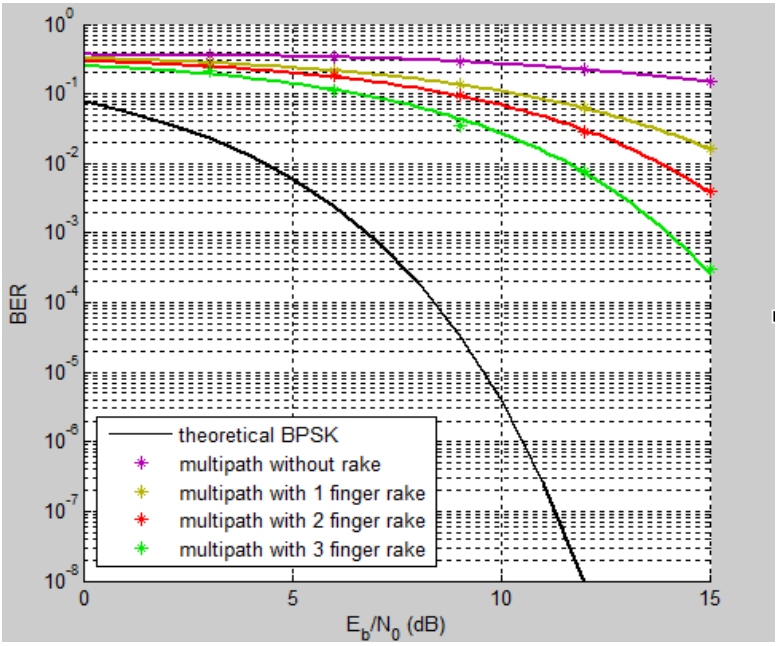

Fig. (4- 16) BER comparison using Hadamard code

(4-4) Phase 3: Testing different combinations of multipath delays

After we developed our model and tested its performance with Rake receiver, next step was to test different combinations of multipath delays to investigate the effect of delay spread. The model structure is the same except for changing the setting values of the delay blocks. We tested 6 different delay combinations for both using PN code and Hadamard code.

(4-4-1) BER Performance

BER plots are shown in figures below for using PN code and Hadamard code respectively. Delay groups used in simulation are [0, 1, 2 chips], [0, 4, 9 chips], [2, 4, 6 chips], [3, 4, 5 chips], [3, 6, 7 chips], [7, 8, 9 chips]. Delay zero refers to direct path. The BER results indicates that the system response changes with the change of the mulipath delay spread and also confirms the last simulation results that PN spreading code has better performance than Hadamard spreading code.

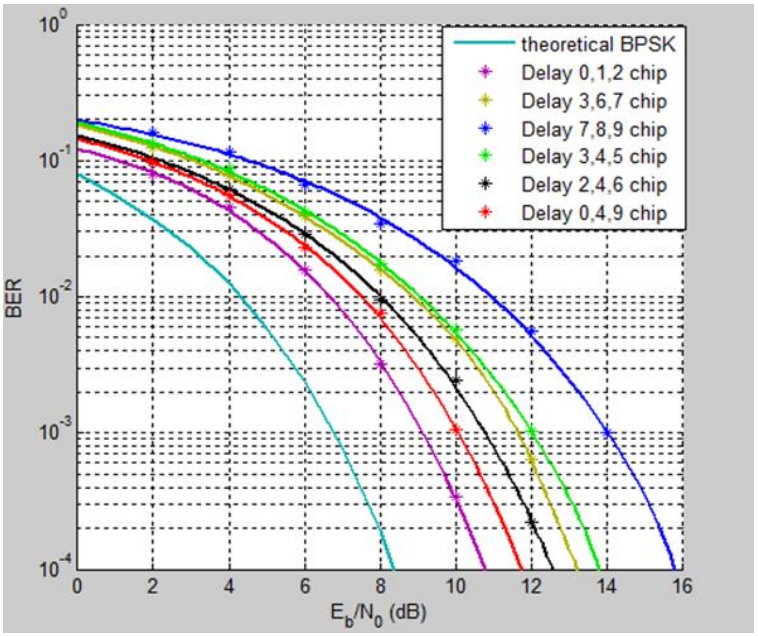

Fig. (4- 17) BER comparison for different delay spreads in case of using PN code

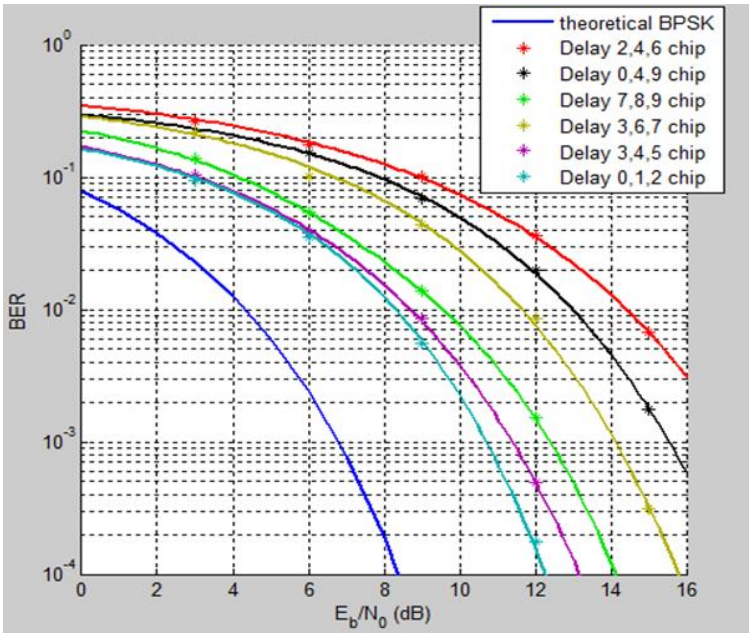

Fig. (4- 18) BER comparison for different delay spreads in case of using Hadamard code

(4-5) phase 4: Providing channel estimation for a stionary channel

In our previous work, we assumed prior knowledge of multipath delays. The next step is to provide delay estimation for the unknown channel using least mean square (LMS) filter. A set of training bits is inserted in the beginning of data transmission to be used by the LMS filter to provide the channel delay estimation. We tested different training sequences with different lengths to choose the one having the best performance to use it in the next step. The sequences used for training were PN sequence, Gold sequence and repeating sequence.

(4-5-1) Matlab model

The following figure shows the matlab model used for implementing phase 4.

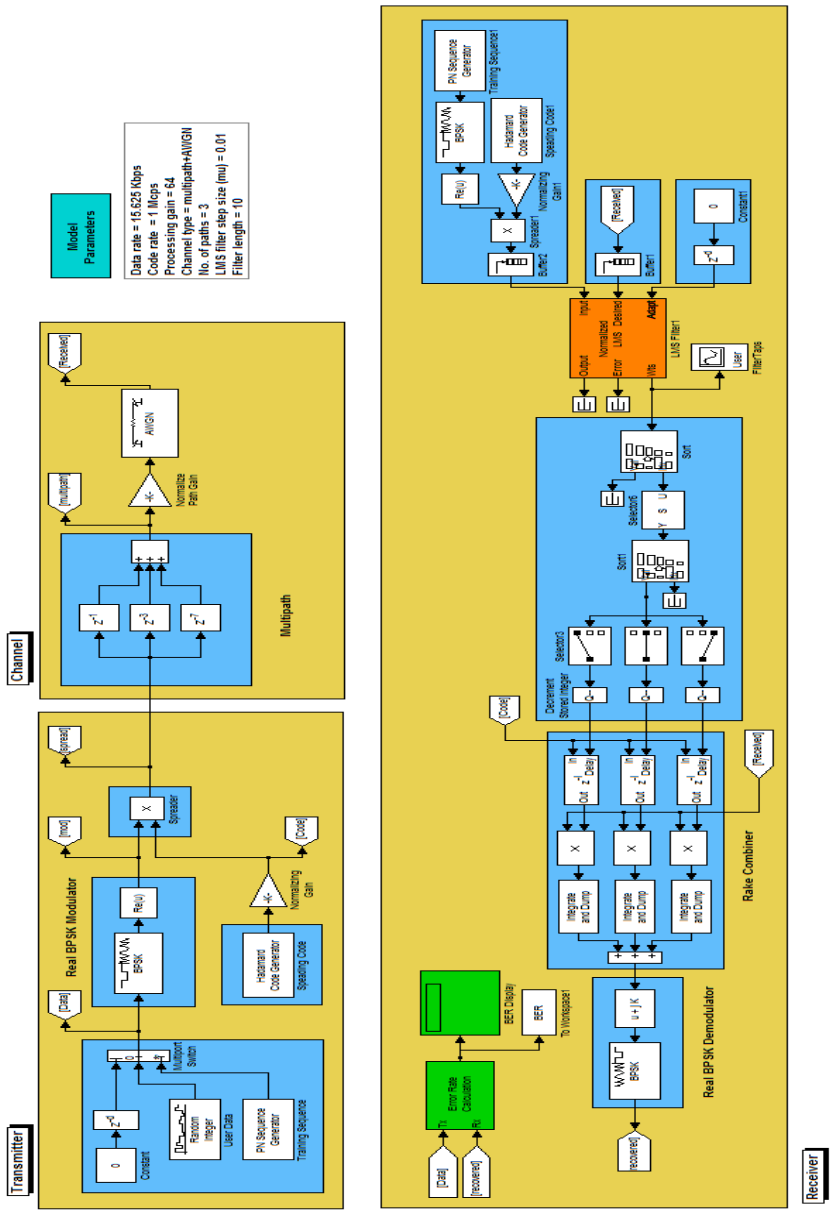

Fig. (4- 19) Matlab model for providing channel delay estimation for a stationary channel

(4-5-2) Exploring the model

i. Generating binary data stream: same as previous model.

ii. ***Generating pilot sequence***: the 3 different sequences mentioned earlier are generated using *PN sequence generator* block, *Gold sequence generator* block and *Repeating sequence stair* block. The pilot sequence is transmitted only once at the beginning of data transmission using *multiport switch* block which Passes through the input signals corresponding to the truncated value of the first input. The first input port is the control port whose input is a zero valued *constant* block which is delayed by a number of bits corresponding to the training sequence length.

iii. ***Generating spreading code****:* by using *Hadamard Code generator* block, which generates a Hadamard Code from an orthogonal set of codes, we got a 64-bit sequence of 1Mcps chip rate. The output code is in a bipolar format with a {0, 1} to {1, -1} element mapping.

iv. ***BPSK modulation****:* same as previous model.

v. ***Spreading****:* same as previous model.

vi. ***Adding multipath****:* same as previous model.

vii. ***Channel delay estimation****:* we used *LMS Filter* block which can implement an adaptive FIR filter using five different algorithms. The block estimates the filter weights, or coefficients, needed to minimize the error between the output signal and the desired signal. We connected the modulated and spreaded training sequence, which we want to filter, to the Input port, and connected the received signal to the desired port. The desired signal must have the same data type, complexity, and dimensions as the input signal. The Output

port outputs the filtered input signal, which is the estimate of the desired signal. The Error port outputs the result of subtracting the output signal from the desired signal. We selected normalized LMS for the Algorithm parameter and the step size is set to 0.01. When the input to Adapt port is greater than zero, the block continuously updates the filter weights and when it is less than or equal to zero, the filter weights remain at their current values. So the input for this port must be greater than zero for certain number of bits that equals the training sequence length used. The Wts port outputs the vector of filter weights. We toke that vector and selected the largest 3 values and calculated their indices which represent the time delay values that will be the inputs for the rake combiner delay blocks.

viii. ***Rake combiner****:* same as previous model except for the delays. We replaced the constant delays with variable ones got from *variable integer delay* block which delays discrete-time input by a time-varying integer number of sample periods specified by the "delay" input. The delay inputs are got from the previous procedure.

ix. ***BPSK demodulation****:* same as previous model.

x. Bit error rate calculation: same as previous model.

xi. ***Results and displays****:* an additional block is used here for displaying the filter taps. We used a *vector scope* block for this purpose.

(4-5-3) Simulation results

This model uses the LMS adaptive FIR algorithm to adaptively estimate the time delays for the noisy distorted received signal. The peak in the filter taps vector indicates the time-delay estimate. This is shown in the following figure. In our model we used multipath delays

of 1, 3 and 7 chips which is Consistent with the result found in the figure below.

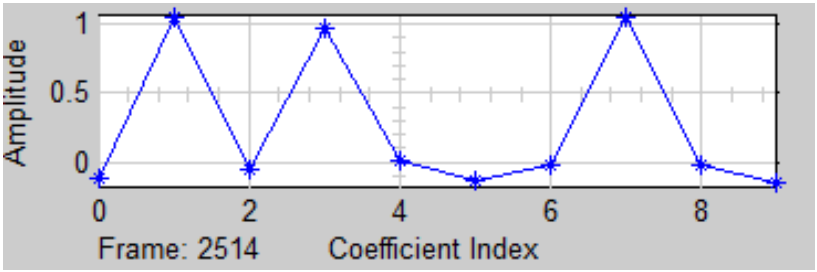

Fig. (4- 20) visualization of filter taps vector

(4-5-4) BER performance

BER plots are shown in figures below for using PN sequence, Gold sequence and repeating sequence respectively as training sequences. Different sequence lengths are tested in each BER session. We used lengths of 4, 8, 16, 32 and 64 bits. The plots indicate that using repeating sequence resulted in better BER performance than the other two sequences.

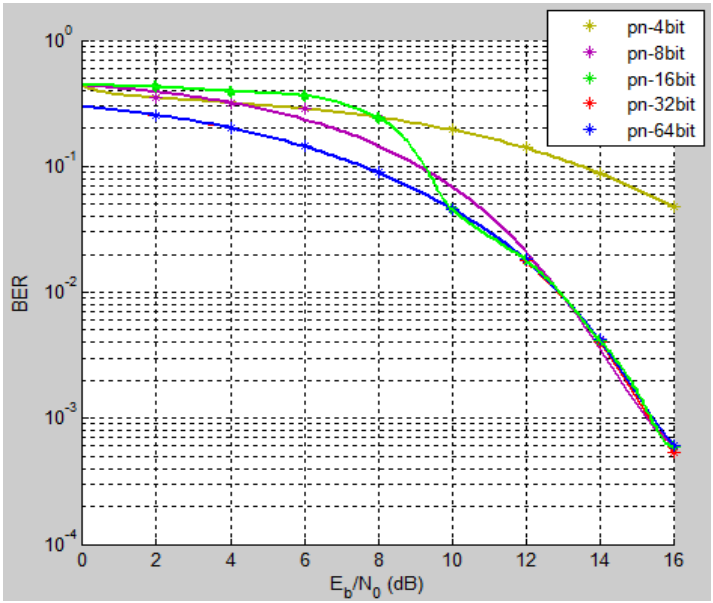

Fig. (4- 21) BER performance for using PN sequence

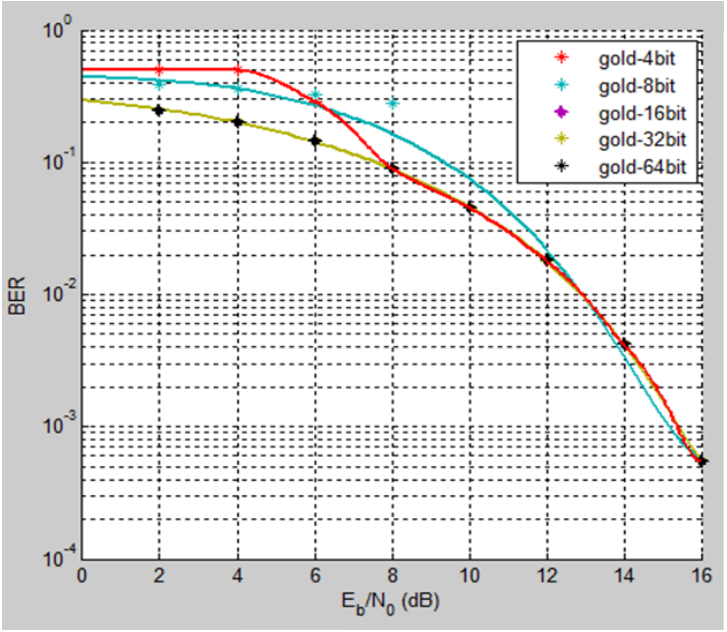

Fig. (4- 22) BER performance for using Gold sequence

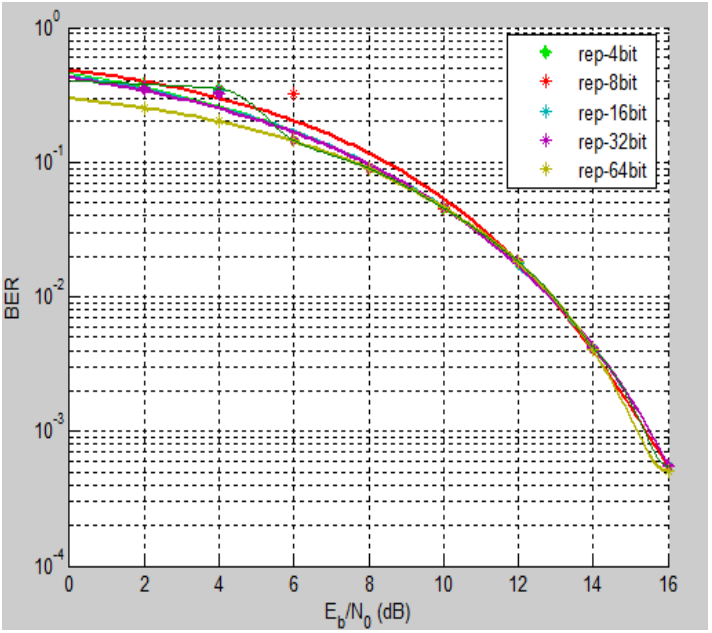

Fig. (4- 23) BER performance for using Repeating sequence

(4-6) phase 5: Using time varying channel

Phase 5 represents the final step in our work. In the previous model, we succeeded in estimating the channel multipath delays for a stationary channel. The new challenge is to provide channel delay estimation for a time varying channel. We modified our model by changing the frame structure of the transmitted data to be 128 bits per frame divided into 2 halves, 64 bits for training sequence and 64 bits for data. This way we can use the training bits sent at any time the channel varies and update the delays estimated. We also changed the channel to a time varying channel by modifying the multipath delays every certain period of time. We tested the model for different variation rates.

(4-6-1) Matlab model

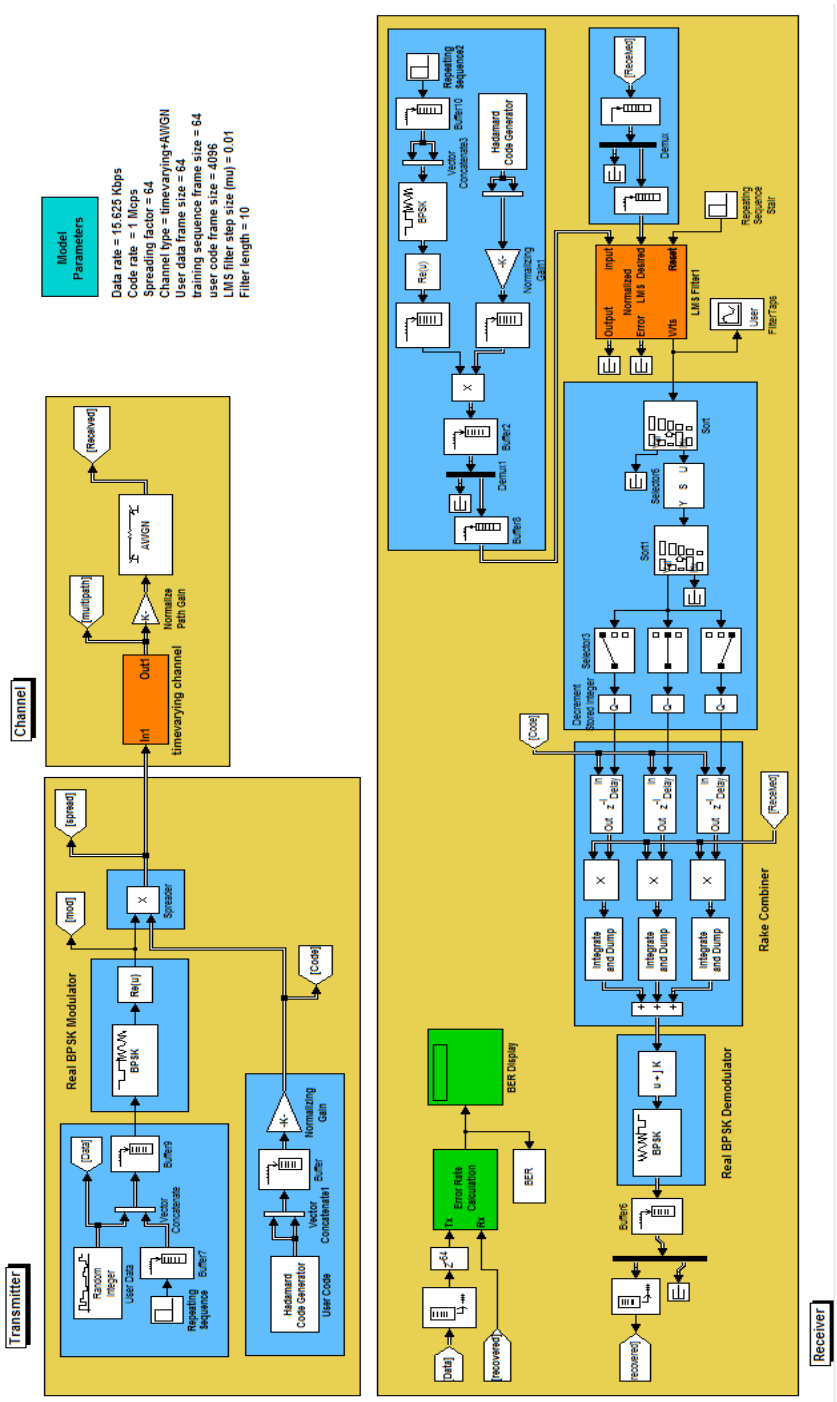

Fig. (4- 24) Matlab model for providing channel delay estimation for a time-varying channel

(4-6-2) Exploring the model

i. ***Generating binary data stream****:* By using *Random integer generator* block and checking the frame-based output option, we generated binary data stream of 15.625Kbps data rate and frame size of 64 bit per frame.

ii. ***Generating pilot sequence***: By using *Repeating sequence stair* block with data rate of 15.625 kbps followed by a *Buffer* block to convert it to frame with size of 64 bits per frame.

iii. ***Concatenation***: To obtain the frame structure needed, we used a *Vector Concatenate* block. This block concatenates input signals of same data type to create contiguous output signal. It shall output a total frame size of 128 bit per frame at data rate of 31.25 kbps.

iv. ***Generating spreading code****:* by using *Hadamard Code generator* block followed by *Vector Concatenate* and *Buffer* blocks, we got a framed Hadamard code of size 8192 bit/frame and data rate of 2Mcps.

v. ***BPSK modulation****:* same as previous model.

vi. ***Spreading****:* same as previous model.

vii. ***Time varying channel****:* we still have a 3 path channel but with some modifications to obtain a channel with a time varying nature. We used *variable integer delay* blocks which delays discrete-time input by a time-varying integer number of sample periods specified by the "delay" input. These delay inputs are random integer inputs with a certain sampling rate which represents the rate of change of the channel. We changed the rate within the range of 0.2sec to 12.8sec.

viii. ***Channel delay estimation****:* we used *LMS Filter* block as in the previous simulation phase but with some modifications in the "Input" and "Desired" input circuits to accommodate with the changes done in the previous procedures. We also replaced the "Adapt" port with "Reset" port. If the Reset port is enabled and a reset event occurs, the block resets the filter weights to their initial values. It is reset in the same time that the channel multipath delays are changed.

ix. ***Rake combiner****:* same as previous model.

x. ***BPSK demodulation****:* same as previous model.

xi. Bit error rate calculation: same as previous model.

xii. ***Results and displays****:* same as previous model.

(4-6-3) BER performance

The BER plot shown demonstrates the different responses of the last model corresponding to the different changing rates of the time varying channel. We have here 8 plots, 6 of them are for testing the model at these rates (0.2s, 0.8s, 1.6s, 3.2s, 6.4s and 12.8s), and 2 of them are for testing the model without using the rake combiner at rates (0.2s and 12.8s). If we compare the BER performance of the system with and without using rake at the same rate, we will see a noticeable improvement in BER after using the rake. On the other hand, the slower the channel changing rate, the better the BER performance. The BER is supposed to be decreasing with the increase in E_b/N_o but at some point, because of residual errors, it looks like constant. This issue needs more investigation and it is recommended for the future work.

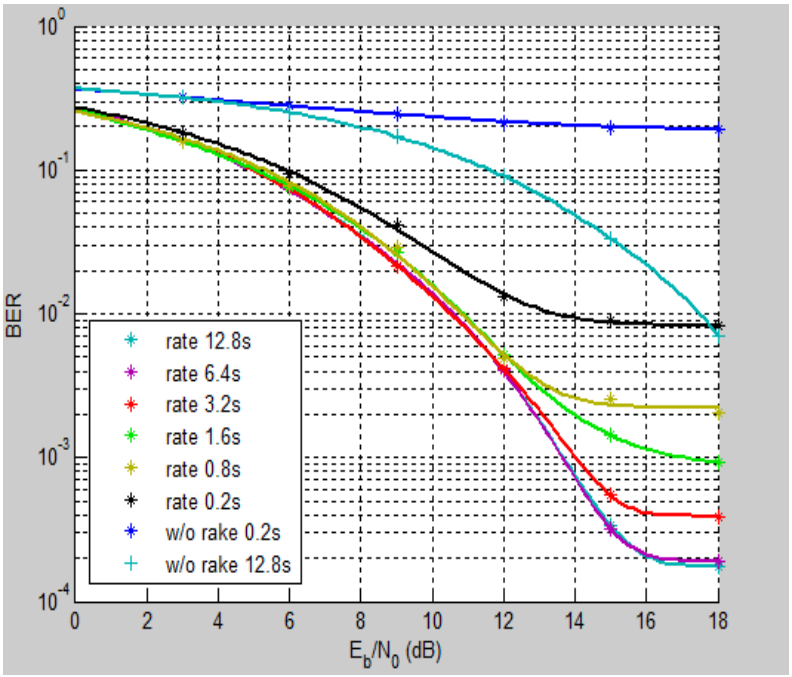

Fig. (4- 25) BER performance for time varying channel model

Chapter 5: Conclusions and Future Work

This chapter concludes the thesis by summarizing important observations, contributions and results. It also highlights the future avenues of research that has originated from the work.

(5-1) Conclusions

This thesis aims to develop a MATLAB model of a spread spectrum system using RAKE receiver and evaluating its performance in a time varying channel. During the course of this research, some theoritical backgrounds were introduced then we followed them by a detailed presentation of our work. A DS-SS system with a BPSK modulation is first introduced and evaluated in AWGN and multipath fading channels with and without Rake receiver. This was performed under different conditions like using different spreading codes and using different number of rake fingers. Ideally, the number of correlators in the RAKE receiver should match the number of multipath signals. The effect of multipath delay spread is then investigated by using different combinations of predefined delays for the multipath channel. The next step was to provide channel estimation using LMS filter for a stationary channel and testing different pilot signals with different lengths. Finally, a complete system was introduced with a time varying channel and tested at different rates of change. The inferred conclusions from this research can be compiled in the following points:

- ✓ Simulation results showed that RAKE receiver is an effective technique for improving spread spectrum systems performance.
- ✓ In multipath fading channel, BER gets better when increasing number of rake fingers.
- ✓ Using different spreading codes exhibits different responses .
- ✓ PN code introduced better BER than Hadamard code since it has better auto-correlation properties.

- ✓ When testing different combinations of multipath delays we found that BER changes with the change in multipath delay spread.
- ✓ LMS filter showed to be a good means of channel delay estimation.
- ✓ Increasing the length of the training sequence improves the BER performance especially when using repeating sequence.
- ✓ The longer the rate that time varying channel changes, the better BER performance .

(5-2) Future Work

Several points can be covered in the future as an extension for this work:

- ☒ Investigation of the impact of channel estimation errors.
- ☒ Expanding the model and taking into account the change in power and phase in the multipath signal.
- ☒ Investigating the performance of the rake receiver using different models of time varying channels.
- ☒ Modeling a multi user scenario.
- ☒ Implementation of RAKE receiver on FPGA.

References

[1] T. S. Rappaport, "*Wireless Communications: Principles and Practice*," Prentice Hall: Upper Saddle River, 2002.

[2] R. Blake, "*Comprehensive Electronics Communication*," West: Minneapolis, 1997.

[3] W. Stallings, "*Wireless Communications and Networks*," Prentice Hall, Upper Saddle River, 2001.

[4] G. A. Bhalerao and R. G. Zope "*BER Improvement of DS-CDMA with Rake Receiver Using Multipath Fading Channel*", International Conference on Recent Trends in engineering & Technology – 2013.

[5] C. H. Yeh, "Multipath Fading Effects on RAKE Receiver Performance Used in Wireless Links thesis", College of graduate studies, Lamar University, May 2001.

[6] R. Price and P. E. Green, "A Communication Technique for Multipath Channels" 1958.

[7] L. Harju *et al*., "*Flexible Implementation of a WCDMA Rake Receiver*", Journal of VLSI signal processing systems for signal, image and video technology January 2005, Volume 39, Issue 1-2, pp 147-160.

[8] M. Chugh *et al*., *"Design and Implementation of Configurable W-CDMA Rake Receiver Architectures on FPGA*", 19th IEEE International Parallel and Distributed Processing Symposium Proceedings, 2005.

[9] V. Jungnickel *et al.*, "*A MIMO RAKE receiver with enhanced interference cancellation*", IEEE 61st Vehicular Technology Conference, 2005.

[10] A. Doukas *et al*., "*Low Complexity Rake Receiver and Channel Estimator Implementation for DSSS-CDMA Systems*", IEEE Ninth

International Symposium on Spread Spectrum Techniques and Applications, 2006.

[11] Y. Yin *et al*., "*A research of UWB rake receiver based on novel RLS adaptive algorithm*", Journal of Electronics (China) May 2006, Volume 23, Issue 3, pp 341-345.

[12] M. Youssef *et al*., "*CodeRAKE: a new small-area scalable architecture for the multi-user/multi-code RAKE receiver*", 13th IEEE International Conference on Electronics, Circuits and Systems, 2006. ICECS '06.

[13] R. J. Chen and C. L. Tsai "*Design and Performance Analysis of the Receivers for DS-UWB Communication Systems*", The IEEE International Conference on Ultra-Wideband, 2006.

[14] W. Quan and A. Dinh " *An N-Selective MRC Rake Receiver with LMS Adaptive Equalizer for UWB Systems*", Canadian Conference on Electrical and Computer Engineering, 2006. CCECE '06.

[15] K. B. Baltzis and J. N. Sahalos " *A Novel Rake Receiver Design for Wideband Wireless Communications*", Wireless Personal Communications, December 2007, Volume 43, Issue 4, pp 1603-1624.

[16] A. Dudkov " *RAKE Reception for Signature-Interleaved DS CDMA in Rayleigh Multipath Channel*" Multi-Carrier Spread Spectrum 2007, Lecture Notes Electrical Engineering Volume 1, 2007, pp 137-145.

[17] D. Cassioli *et al*., " *Low Complexity Rake Receivers in Ultra-Wideband Channels*", IEEE Transactions on Wireless Communications, 2007.

[18] K. Ouertani et al., "Performance Comparison of RAKE and SIC/RAKE Receivers for Multiuser Underwater Acoustic Communication Applications", OCEANS 2007 – Europe.

[19] C.C. Tsimenidis et al., " Adaptive Spread-Spectrum based RAKE Receiver for Shallow-Water Acoustic Channels", OCEANS 2007 – Europe.

[20] J. He and M. Salehi, "A *new finger placement algorithm for the Generalized RAKE receiver*", 42nd Annual Conference on Information Sciences and Systems, CISS 2008.

[21] A. Sagahyroon *et al*., "*An FPGA Implementation of the Searcher Algorithm*",4th IEEE International Symposium on Electronic Design, Test and Applications, DELTA 2008.

[22] K. S. Chaitanya, *et al*., "*Implementation of CORDIC based RAKE receiver architecture*", 2nd IEEE International Conference on Computer Science and Information Technology, ICCSIT 2009.

[23] C. Thomos, and G. Kalivas, " *FPGA-based architecture of a DS-UWB Channel Estimator and RAKE Receiver employing a hybrid selection scheme*", IEEE 17th International Conference on Telecommunications (ICT), 2010.

[24] L. Qi *et al*., "*A Novel Rake Receiver Using RLS Adaptive Algorithm for DS-UWB Systems*", 6th International Conference on Wireless Communications Networking and Mobile Computing (WiCOM), 2010.

[25] S. H. Choudhury, et al., "A New Approach in the Modeling of an MC-CDMA RAKE Receiver and Its Performance Evaluation under the Effect of Multipath Fading Channel", International Conference on Computational Intelligence and Communication Networks (CICN), 2010.

[26] H. yang Fu *et al*., "*Performances comparison among smart antenna RAKE receiver and the other applicable RAKE receivers*", The 12th International Conference on Advanced Communication Technology (ICACT), 2010 (Volume: 2).

[27] R. Prasad, "*CDMA for Wireless Personal Communications*," Artech House, Boston, 1996.

[28] S. Haykin, "*Communication systems*," John Wiley & Sons, Inc. 4th edition, 2001.

[29] K. Fazel and S. Kaiser, "*Multi-Carrier and Spread Spectrum Systems*," John Wiley & Sons, 2003.

[30] R. E. Zeimer and R. L. Peterson, "*Digital Communications and Spread Spectrum Systems*," New York: Macmillan, 1985.

[31] A. J. Viterbi, " *CDMA: Principles of Spread Spectrum Communication*," Reading, MA: Addison-Wesley, 1995.

[32] Application Note 1890, "*An Introduction to Spread-Spectrum Communications*," http://www.maxim-ic.com/an1890, 2003.

[33] R. Pickholtz, D. Schilling, and L. Milstein, "*Theory of Spread-Spectrum Communications - A Tutorial*" IEEE Trans. Comm., vol. COM 30, pp. 855-884, May 1982 .

[34] ir. J. Meel, " *Spread Spectrum (SS)*, " DE NAYER Institute , 1999.

[35] T. Darwich and C. Cavanaugh, "*Amplitude Shifting for Sidelobes Cancellation pulse compression*," Technical Report TR-2006-4-001, Center for Advanced Computer Studies University of Louisiana, May 2006.

[36] R. E. Ziemer , "*Fundamentals of Spread Spectrum Modulation*," University of Colorado at Colorado Springs, 2007.

[37] A. Mitra "*On Pseudo-Random and Orthogonal Binary Spreading Sequences*", International Journal of Information and Communication Engineering 4:6 2008.

[38] G. Giunta , "*Basic note on Spread Spectrum CDMA signals*," for the academic course of *Digital Signal Processing* of the Third University of Rome, May 2000.

[39] A. Goldsmith**,** "*Wireless Communication*," Stanford University, 2004.

[40] H. Hara and R. Prasad, "*Overview of multicarrier CDMA*," *IEEE* Communications Magazine, vol. 35, pp. 126–133, Dec. 1997.

[41] J. W. Ketchum and J. G. Proakis, "Adaptive algorithms for estimating and suppressing narrow band interference in PN spread spectrum systems," IEEE Transactions on Communications, vol. 30, pp. 913–924, May 1982.

[42] L. B. Milstein, "*Interference rejection techniques in spread spectrum communications*," Proceedings of the *IEEE*, vol. 76, pp. 657–671, June 1988.

[43] R. Esmailzadeh and M. Nakagawa, "*TDD-CDMA for Wireless Communications*," Artech House, 2003.

[44] Valery P. Ipatov, "*Spread Spectrum and CDMA Principles and Applications*," University of Turku, Finland, John Wiley & Sons, 2005.

[45] G. L. Turin, "Introduction to Spread Spectrum Anti Multipath Techniques and Their Application to Urban Digital Radio," IEEE Proc., Vol. 68, No. 3, March 1980, pp.328–353.

[46] M. K. Simon, et al., "*Spread Spectrum Communications*," Rockville, MD: Computer Science Press, 1985.

[47] M. Blanco and K. Zdunek, "Performance and optimization of switched diversity systems for the detection of signals with rayleigh fading," IEEE Trans. Commun., pp. 1887–1895, Dec. 1979.

[48] M. Simon and M.-S. Alouini, "Digital Communication over Fading Channels A Unified approach to Performance Analysis," Wiley, 2000.

[49] M. Yacoub, "Principles of Mobile Radio Engineering," CRC Press, 1993.

[50] G. L. Stuber, "*Principles of Mobile Communications*," *2nd Ed.* Kluwer Academic Publishers, 2001.

[51] D. Torrieri, "*Principles Of Spread Spectrum Communication Systems*", Springer Science + Business Media, Inc. 2005.

[52] http://en.wikipedia.org/wiki/Rake_receiver.

[53] S. P. Gan, "*CDMA Detection Guided RAKE Receiver thesis,"* University of Queensland, oct 2002.

[54] F. H´eliot, "Design and Analysis of Space-time Block and Trellis Coding Schemes for Single-Band UWB Communications Systems thesis," King's College London, May 2006.

[55] J. G. Proakis, "Digital Communications", McGraw Hill Inc., 1995.

[56] F. Ling, "Coherent detection with reference symbol based estimation for direct sequence CDMA uplink communication," in Proc. of IEEE VTC'93, (New Jersy. USA), pp.400-403, May 1993.

[57] S. Tantikovit et al., "The effect of channel estimation, interleaving and channel coding on Rake receivers for mobile DS-CDMA systems," in Proc. of IEEE VTC'99, pp.2422-2426, 1999.

[58] S. KO and H. Choi, "Effect of imperfect channel estimation on the performance of pilot channel-aided coherent DS-CDMA system over Raileigh fading multipath channel," IEICE Trans. On Commun., vol. E83-B, pp. 721-733, March 2000.

[59] M. S. Alouini *et al*., "*Rake reception with maximal ratio and equal gain combining for DS-CDMA systems in Nakagami fading*," in proc. Of 6th IEEE International Conf. on Universal Personal Communications Record, vol. 2, pp. 708-712, Oct. 1997.

[60] S. Haykin, "*Adaptive filter theory*," Prentice Hall, 3rd ed., 1996.

[61] J. G. Proakis, "*Adaptive equalization for TDMA digital mobile radio*," IEEE Trans. Veh. Techno., vol. 40, pp. 333-341, May 1991.

[62] S. A. Fechtel and H. Meyer, "*Optimal parametric feedforward estimation of frequency selective fading radio channels*," IEEE Trans. Commun., vol. 42, pp. 1639-1650, Feb/March/April 1994.

[63] M. Tsatsanis and G. B. Giannakis, "*Estimation and equalization of fading channels with random coeffecients*," Signal Processing, vol. 53, Sept. 1996.

[64] D. K. Borah and B. Hart, "Frequency selective fading channel estimation with a polynomial time varying channel model," IEEE Trans. Commun., vol 47, pp. 862-873, June 1999.

[65] F. R. Magee and J. G. Proakis, "Adaptive maximum likelihood sequence estimation for digital signaling in the presence of intersymbol interference," IEEE Trans. Info. Theory, vol. IT-19, pp. 120-124, Jan. 1973.

[66] O. Macchi and N. J. Bershad, "*Adaptive recovery of a chirped sinusoid in noise part I: Performance of the RLS algorithm*," IEEE Trans. Acoust., Speech, Signal Processing, vol. 39, pp. 583-594, March 1991.

[67] O. Macchi and N. J. Bershad, "*Adaptive recovery of a chirped sinusoid in noise part II: Performance of the LMS algorithm*," IEEE Trans. Acoust., Speech, Signal Processing, vol. 39, pp. 595-602, March 1991.

[68] B. Widrow and S. D. Stearns, "*Adaptive Signal Processing*," Prentice Hall: New Jersey. 1985.

[69] J. Homer et al., "*LMS estimation via structural detection*," IEEE Transactions on Signal Processing, 46(10): 2651-2663. 1998.

[70] J. Homer, "*A review of the developments in adaptive echo cancellation for telecommunications*," Journal of Electrical and Electronics Engineering, Australia, 18(2): 149-164. 1998.

[71] Homer, J., Bitmead, R.R., & Mareels, I. 1998. Quantifying the effects of dimension on the convergence rate of LMS adaptive FIR estimator. IEEE Transactions on Signal Processing, 46 (10): 2611-2615.

[72] Homer, J. 2000. Detection guided NLMS estimation of sparsely parametrized channels. IEEE Transactions on Circuits and Systems-II: Analog and Digital Signal Processing, 47(12): 1437-1442.

[73] B. Elbert and M. Schiff, "*Simulating the Performance of Communication Links with Satellite Transponders*," Application Technology Strategy, Elanix, Inc.

الملخص العربى

فى بيئة اللاسلكى تصل الاشارات المنقوله الى جهاز الاستقبال عن طريق المسار المباشرغير المعاق او عن طريق المسارات المتعددة من الانعاكس او الحيود او الانتشار من العناصر المحيطة. هذا المسار المتعدد يسبب تشوه واضمحلال ملحوظ للاشارة لدى المستقبل مما يؤدى الى تداخل بين الرموز و تستخدم انظمة الطيف المنتشر المستقبلات المجمعة لتقليل اخطاء الاتصال الناتجة من تأثير المسار المتعدد عن طريق تجميع الطاقة من المسارات الواضحه.

الغرض من هذا البحث هو تقديم نموذج بالماتلاب لنظام الطيف المنتشر متضمنا المستقبل المجمع وتقييم اداءه فى قنوات متغيرة الزمن. فى البداية يتم تقديم نظام الانتشار الطيفى التتابعى المباشر باستخدام تعديل طور التناوب الثنائى وتقييم أدائه فى قناة ضجيج جاوس المضاف وقنوات الخفوت متعدد المسارات فى وجود المستقبل المجمع وفى عدم وجوده. يتم تنفيذ هذا تحت شروط مختلفة كاستخدام شفرات انتشار مختلفة واستخدام عدد مختلف من اصابع المجمع. نظريا، عدد أصابع المستقبل المجمع يجب ان يماثل عدد الاشارات متعددة المسارات. يتم بعد ذلك دراسة تأثير الانتشار المتأخر متعدد المسارات باستخدام تركيبات مختلفة من التأخيرات المعرفة مسبقا لقناة متعددة المسارات. الخطوة التالية هى تخمين القناة باستخدام فلتر المربع المتوسط الأدنى لقناة ثابتة واختبار اشارات ارشادية مختلفة بأطوال مختلفة. فى الختام، يتم تقديم نظام متكامل من خلال قناة متغيرة الزمن واختبارها عند معدلات تغيير مختلفة. يتم تقييم أداء النظام المحاكى عن طريق حساب معدل الخطأ باستخدام تحليل مونت كارلو والتحليل النظرى المدعم من برنامج الماتلاب اصدار (7.8).

تتكون هذه الرسالة من خمسة فصول مقسمة كالأتى :

الفصل التمهيدى يعرض مقدمة مختصرة عن خصائص انتشار الاشارات فى قناة الراديو اللاسلكية وكيف ان الموجة المحصلة يمكن ان تتشوه بشدة والحاجة الى استخدام المستقبل المجمع، ودراسة مفصلة عن الابحاث السابقة.

الفصل الثانى يشرح المفهوم الأساسى ومبادئ تقنية الانتشار الطيفى، الانواع المختلفة من شفرات الانتشار وخصائصها ، ومبادئ تعديل الانتشار الطيفى التتابعى المباشر.

الفصل الثالث يحتوى على مفهوم التباين وانواعه المختلفة، تقنيات الدمج المختلفة وأدائها، مبدأ المستقبل المجمع وكيفية عمله، ومبدأ خوارزيم المربع المتوسط الأدنى ودوره فى تخمين تأخير القناة.

الفصل الرابع يقدم تسلسل محاكاة العمل متضمنا نماذج الماتلاب التفصيلية ، نتائج المحاكاة، ومقارنات معدل الخطأ.

الفصل الخامس يقدم للقارئ ملخص كلى للنتائج المجمعة ، الاستنتاجات والتوصيات المقترحة والتحسينات التى يمكن عملها مستقبلا فى هذا الموضوع.

تحسين الاشارات الرقمية فى القنوات متغيرة الزمن باستخدام المستقبل المجمع

رسالة مقدمة من

أمل صبرى فرج الله حجازى

إلى كلية الهندسة ببنها -جامعة بنها

كجزء من متطلبات الحصول على درجة ماجستير الهندسة والتكنولوجيا في تكنولوجيا الهندسة الكهربية من كلية الهندسة ببنها

اعتمدت وأجيزت من السادة الممتحنين

أ.د./ عبدالحليم عبدالنبى ذكرى **(مشرفاً ورئيساً)**
أستاذالالكترونيات والاتصالات، كلية الهندسة، جامعة عين شمس .....

أ.د./ طلعت عبداللطيف الجرف **(ممتحنا خارجياً و عضواً)**
أستاذ الاتصالات بالمعهد التكنولوجى العالى بالعاشر من رمضان .....

أ.د./ صلاح غازي رمضان **(ممتحناً داخلياً وعضواً)**
أستاذ متفرغ بقسم الهندسة الكهربية، كلية الهندسة ، جامعة بنها .....

اعتمدت من قسم تكنولوجيا الهندسة الكهربية **(رئيس القسم)**
أ.د./ محمود الباهي .....

اعتمدت من الدراسات العليا **(وكيل الكلية للدراسات العليا)**
أ.د./ هشام البطش .....

اعتمدت من كلية الهندسة ببنها **(عميد الكلية)**
أ.د./ محمد بسيوني .....

كلية الهندسة

جامعة بنها

تحسين الاشارات الرقمية فى القنوات متغيرة الزمن باستخدام المستقبل المجمع

رسالة مقدمة من

أمل صبرى فرج الله حجازى

كجزء من
متطلبات الحصول على درجة
الماجستير
فى
تكنولوجيا الهندسة الكهربية

تحت اشراف

أ.د. عبدالحليم عبدالنبى ذكرى
قسم هندسة الالكترونيات والاتصالات
كلية الهندسة
جامعة عين شمس

د. أيمن مصطفى حسن
قسم الهندسة الكهربية
كلية الهندسة
جامعة بنها

د. حسام الدين السيد
قسم الهندسة الكهربية
كلية الهندسة
جامعة بنها

سبتمبر 2013